Accepted Manuscript

Novel gold(I) complexes with 5-phenyl-1,3,4-oxadiazole-2-thione and phosphine as potential anticancer and antileishmanial agents

Joana Darc S. Chaves, Luiza Guimarães Tunes, Chris Hebert de J. Franco, Thiago Martins Francisco, Charlane Cimini Corrêa, Silvane M.F. Murta, Rubens Lima Monte-Neto, Heveline Silva, Ana Paula S. Fontes, Mauro V. de Almeida

PII: S0223-5234(16)30914-X

DOI: 10.1016/j.ejmech.2016.10.052

Reference: EJMECH 9017

To appear in: *European Journal of Medicinal Chemistry*

Received Date: 9 May 2016

Revised Date: 21 October 2016

Accepted Date: 22 October 2016

Please cite this article as: J.D.S. Chaves, L.G. Tunes, C.H. de J. Franco, T.M. Francisco, C.C. Corrêa, S.M.F. Murta, R.L. Monte-Neto, H. Silva, A.P.S. Fontes, M.V. de Almeida, Novel gold(I) complexes with 5-phenyl-1,3,4-oxadiazole-2-thione and phosphine as potential anticancer and antileishmanial agents, *European Journal of Medicinal Chemistry* (2016), doi: 10.1016/j.ejmech.2016.10.052.

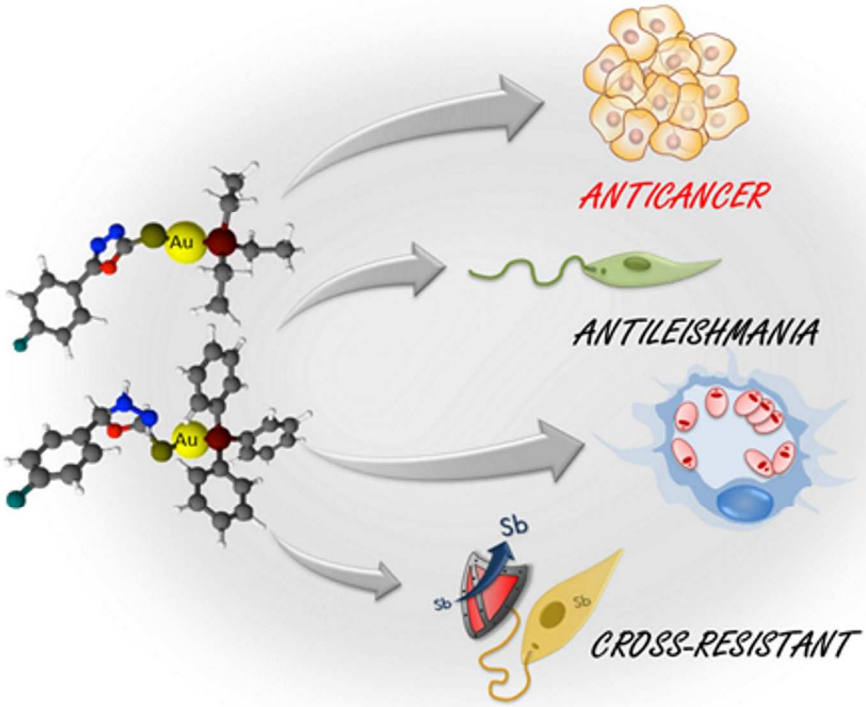

Novel gold(I) complexes with 5-phenyl-1,3,4-oxadiazole-2-thione and phosphine as potential anticancer and antileishmanial agents

Joana Darc S. Chaves[a], Luiza Guimarães Tunes[b], Chris Hebert de J. Franco[a], Thiago Martins Francisco[c], Charlane Cimini Corrêa[a], Silvane M. F. Murta[b], Rubens Lima Monte-Neto[b], Heveline Silva[d], Ana Paula S. Fontes[a], Mauro V. de Almeida[a]*

[a]Departamento de Química, ICE, Universidade Federal de Juiz de Fora, 36036-330. Juiz de Fora, MG, Brazil

[b]Centro de Pesquisas René Rachou – Fundação Oswaldo Cruz, 30190-002. Belo Horizonte, MG, Brazil

[c]Departamento de Física, Universidade Federal de Minas Gerais, 31270-901. Belo Horizonte, MG, Brazil

[d]Departamento de Química, Universidade Federal de Minas Gerais, 31270-901. Belo Horizonte, MG, Brazil

*Correspondingauthor. Fax +55 32 21023310[1]

E-mail address: mauro.almeida@ufjf.edu.br (M. V. de Almeida)

***Abbreviations*:** AmB, Amphotericin B; α-MEM, minimum essential medium; BHK-21, Hamster (*Mesocricetus auratus*) kidney fibroblast; B16-F10, mouse (*Mus musculus*) skin melanoma cell line; CT26.WT, mouse (*Mus musculus*) colon cancer fibroblast cell line; DMSO, dimethylsulfoxide; FBS, fetal bovine serum; HRMS(ESI), high-resolution mass spectra (electrospray ionization); HYG, hygromycin B phosphotransferase encoding gene; IR, infrared; LUC, firefly luciferase encoding gene; MIL, miltefosine; MTT, thiazolyl blue tetrazolium bromide; NMR, nuclear magnetic resonance; pSP72, cloning vector; RPMI, roswell park memorial institute culture medium; TMS, tetramethylsilane

Abstract

The current anticancer and antileishmanial drug arsenal presents several limitations concerning their specificity, efficacy, costs and the emergence of drug-resistant cells lines, which encourages the urgent need to search for new alternatives. Inspired by the fact that gold(I)-based compounds are promising antitumoral and antileishmanial drug candidates, we synthesized novel gold(I) complexes containing phosphine and 5-phenyl-1,3,4-oxadiazole-2-thione and evaluated their anticancer and antileishmanial activities. Synthesis was performed by reacting 5-phenyl-1,3,4-oxadiazole-2-thione derivatives with chloro(triphenylphosphine)gold(I) and chloro(triethylphosphine)gold(I). The novel compounds were characterized by infrared, Raman, ^{1}H, ^{13}C nuclear magnetic resonance, high-resolution mass spectra, and x-ray crystallography. The coordination of the ligands to gold(I) occurred through the exocyclic sulfur atom. All gold(I) complexes were active at low micromolar or nanomolar range with IC_{50} values ranging from <0.10 to 1.66 μM against cancer cell lines and from 0.9 to 4.2 μM for *Leishmania infantum* intracellular amastigotes. Compound (**6-A**) was very selective against murine melanoma B16F10, colon cancer CT26.WT cell lines and *L. infantum* intracellular amastigotes. Compound (**7-B**) presented the highest anticancer activity against both cancer cell lines while the promising antileishmanial lead was compound (**6-A**). Tiethylphosphine gold(I) complexes were more active than the conterparts triphenylphosphine derivatives for both anticancer and antileishmanial activities. Triethylphosphine gold(I) derivatives presented antimony cross-resistance in *L. guyanensis* demonstrating their potential to be used as chemical tools to better understand mechanisms of drug resistance and action. These findings revealed the anticancer and antileishmanial potential of gold(I) oxadiazole phosphine derivatives.

Keywords: Gold(I) complexes; 5-Phenyl-1,3,4-oxadiazole-2-thione; antitumor activity; antileishmania

1. Introduction

Cancers and leishmaniasis are considered a spectrum of diseases that can affect different tissues on mammalian hosts. Classified as neglected tropical disease, leishmaniasis is caused by obligate intracellular protozoan parasites of the genus *Leishmania* which causes clinical manifestations as visceral, cutaneous, mucocutaneous and diffuse leishmaniasis – depending on tropism, parasite species and host immunological status. In a similar way, clinical cancer manifestations are diverse with more than hundred types of different cancers [1]. Both diseases are considered a serious global public health problem. It is estimated that leishmaniasis is responsible for 20,000 to 40,000 deaths annually [2] while cancer is a leading causing of death worldwide contributing to 15% of all deaths, with total of 8.2 million in 2012 [3]. *Leishmania* parasites and cancer cells share similar cellular and molecular features such as specific tissue tropisms, metastasis, evasion of the immune system, multifactorial drug resistance mechanisms, high rates of cell proliferation and genome plasticity (genomic rearrangements, gene deletion, insertion, mutation and gene copy number variations) [1, 4]. Curiously, miltefosine, an alkylphosphocholine drug originally developed to treat cancer is the only oral drug used for more than 15 years in India to treat visceral and cutaneous leishmaniasis [5]. An example of drug repurposing that inspired several alternative chemotherapeutic schemes.

Chemotherapy is the major strategy to treat both leishmaniasis and cancers, despite its drawbacks such as limited efficacy and safety, high costs and the emergence of drug resistant cells, which encourage the urgent search for new drugs alternatives. The available drug arsenal against leishmaniasis is limited and the emergence of drug resistant *Leishmania* strains justifies the urgent search for new alternatives. Metal-based drugs are promising antileishmanial agents. For example, Cu(II), Ni(II) and Co(II) triazopyrimidine derivatives were active against intracellular *L. braziliensis* amastigotes and presented *in vivo* efficacy against the *Leishmania* related trypanosomatid *Trypanosoma cruzi*, reducing parasitemia in in 83% [6]. Ni(II) thiourea and Co(II) acyl thiourea complexes were also highly active against both *L. major* and lung carcinoma cell line H-157, with potency in the nanomolar range [7, 8]. Cisplatin, a platinum-based DNA biding drug was active against experimental murine visceral leishmaniasis being able to reduce parasite load in 75% [9]. Several gold(I) and gold(III) derivatives are antileishmanial agents acting as DNA intercalators [10] or by inhibiting kinetoplastid

parasite-specific enzymes NADH fumarate reductase [11], cysteine proteases [12] and TryR [13, 14].

Gold-based compounds are thiophilic agents recognized by their anti-inflammatory properties and have been shown as promising anticancer [15-17] and antileishmanial agents [18]. Solganol, myochrysine and auranofin are gold(I)-derived compounds used to treat rheumatoid arthritis being the latter – a triethylphosphine gold(I) complex – able to inhibit reductase enzymes essential to redox homeostasis in cancer cells and parasites, including *Leishmania* [13, 19-21]. Known to exhibit antitumoral activity even against cisplatin-resistant tumor cells [22, 23], auranofin is currently under clinical trials against several types of cancers [24]. Besides the known anticancer and antileishmanial activity, gold(I) and gold(III) complexes also present antiparasitic activities against *Plasmodium*, *Schistosoma* and other Trypanosomatids such as *Trypanosoma cruzi* and *T. brucei* [25, 26].

Gold(III) compounds share electronic and steric features with platinum(II) which make them alternative anticancer candidates to circumvent platinum associated drawbacks such as resistance and side effects by targeting proteins instead of DNA [27]. Gold(III) compounds act as prodrugs being reduced *in vivo* to their metabolite gold(I) active form [28], showing the importance of biotransformation on its pharmacokinetics and pharmacodynamics. Gold-based complexes can display a plethora of targets due to the structural diversity of ligands and their resulted complexes. Indeed, the mode of action of gold compounds can include: cell cycle alteration; generation of reactive oxygen species that could lead to mitochondrial and/or DNA damages; proteasome inhibition; thioredoxin reductase inhibition and topoisomerase IB inhibition, all leading to apoptosis [26]. The high affinity of gold-based compounds for selenoproteins and thiol-containing proteins makes them powerful drug candidates targeting important enzymes involved in redox homeostasis [28].

In addition to the rational drug design of gold(I) complexes, heterocyclic compounds containing five-membered rings gained importance because of their versatile biological properties. In particular, compounds bearing 1,3,4-oxadiazole moiety have been found to potentiate antimicrobial [29] and anticancer activities [30] which has attracted attention of the chemist in the search for new therapeutic molecules. Oxadiazole is considered to be derived from furan by replacement of two methane (-CH=) group by two pyridine nitrogen (-N=) [31]. The synthesis of gold complexes containing 1,3,4-oxadiazoles is of considerable interest due to their potential biological

activities such as antimicrobial [32], analgesic, anti-inflammatory, anti-HIV [31], antitumoral [33], herbicidal [34], anti-depressive, anti-Parkinson, and anticonvulsant activities [35, 36]. In the course of our studies on gold(I) compounds, we recently synthesized two gold(I) complexes with 5-phenyl-1,3,4-oxadiazole-2-thione and phosphine, which have been shown to be potential antitumor candidates [37].

Inspired by the promising properties of gold(I)-based 1,3,4-oxadiazole derivatives, here we report the synthesis, characterization and investigate the *in vitro* anticancer and antileishmanial activity of eight novel gold(I) complexes containing 5-phenyl-1,3,4-oxadiazole-2-thione and phosphine.

2. Results and discussion

A series of gold(I) triphenylphosphine and triethylphosphine complexes with ligands derivatives 5-(phenyl)-1,3,4-oxadiazole-2-thione containing different substituents in position five of the aromatic ring (Scheme 1 – experimental section) were synthesized by reaction of $Au(PEt_3)Cl$ or $Au(PPh_3)Cl$ and the corresponding ligand in dichloromethane/acetone 1:1, at room temperature, and were isolated by preparative plate chromatography.

The compounds were characterized using a combination of several methods that included ^{1}H NMR, ^{13}C NMR, infrared, Raman, high-resolution mass spectra and single crystal X-ray diffraction for ligand (**D**) and complexes (**3-C**, **4-D**, **5-E** and **8-C**). The complexes are insoluble in water and soluble in dichloromethane, DMSO and present a high chemical stability in organic solvent mixtures.

Ligands (**A**-**E**) can display two tautomeric forms (Y) and (Z), Scheme 2 (Experimental section).The existence of these tautomeric forms has been reported in the literature [38-42]. Spectroscopic evidence suggested that the free ligands are present in the thione tautomeric form (Y). X-ray diffraction data showed that in complexes the ligands are in the thiolate form (Z).

2.1 Vibrational spectra

The absorption corresponding to νSH at 2567-2615 cm^{-1} was not observed in the infrared and Raman spectra of ligands and complexes. We can observe an absorption band in the spectra of the free ligands corresponding to νNH in the range of 3090-3209 cm^{-1} and characteristic thioamide bands νNC=S at ~1300-1347 cm^{-1} [43] indicating that

they are present in the tautomeric form (Y) which was confirmed by X-ray diffraction data obtained for ligand (**D**).

The infrared spectra of all the complexes have shown the absence of νSH, νNH and νC=S bands and the appearance of new bands at 689-710 cm^{-1} attributed to νCS, indicating the formation of the complexes. Figure S1 shows infrared spectra of ligand (**C**), and gold complexes (**3-C** and **8-C**).

Raman spectra of all the complexes exhibited low intensity bands around 250-340 cm^{-1} and 360-390 cm^{-1} which may be attributed to νAu-S and to νAu-P, respectively [44-46].

2.2 NMR studies

In the ^{1}H NMR spectra of complexes, (Scheme 1) the signals of all aromatic hydrogen atoms undergo shifts compared to their positions in the free ligands in the order of 0.2-0.4 ppm. It is also noted in the ^{1}H NMR spectra of complexes (**1-A**, **2-B**, **3-C**, **4-D** and **5-E**) the appearance of a signal in the δ 7.53-7.66 ppm region corresponding to aromatic hydrogen atoms of the PPh_3 group. For complexes (**6-A**, **7-B**, **8-C**, **9-D** and **10-E**) two signals were observed in the regions: δ 1.12-1.24 ppm (CH_3) and δ 1.94-2.06 ppm (CH_2) corresponding to hydrogen atoms from PEt_3 group.

In the ^{13}C NMR spectra of complexes is observed a chemical shift to lower frequency for carbon (C2) due to the presence of the gold and a chemical shift to higher frequency for the carbon atom C5, when compared to the spectra of the free ligands. Table S1 shows the ^{13}C chemical shifts (δ) of the ligands and their complexes
and Figures S2 and S3 show representative ^{1}H NMR and ^{13}C NMR spectra of ligand (**D**), and gold complexes (**4-D**) and (**9-D**).

2.3 X-ray structural determination

Single crystals of ligand (**D**) and complexes (**3-C**, **4-D**, **5-E** and **8-C**) were obtained by recrystallization from a mixture of dimethylsulfoxide and dichloromethane and isolated by filtration. The structure of (**D**) and complexes (**3-C**, **4-D**, **5-E** and **8-C**) were determined using single-crystal X-ray diffraction (Fig. 1 and Fig. 2). Crystal and collection data and structure refinement details are summarized in Tables 1 and 2.

The resolution of the crystal structure of the ligand (**D**) clearly shows the predominance of the thione form. It can be verified by the presence of a hydrogen atom

on N1 and the distance S1-C = 1.643(2) Å. One molecule of the solvent DMSO is present in the crystal lattice of the ligand (**D**).

Insert fig. 1

Insert fig. 2

Insert Table 1

Insert Table 2

Complexes (**3-C**), (**4-D**) and (**8-C**) present two crystallographically independent units of Au-ligand. The ligand 5-phenyl-1-(4-fluoro)-1,3,4-oxadiazole-2-thiol is coordinated by the sulfur atom to the central metal ion, gold(I). The coordination sphere deviates slightly of the linear geometry that is completed with a tertiary phosphine (PPh_3 or PEt_3). The bond angle for complex (**3-C**) is P1A-Au1A-S1A = 168.93(3)° and P1-Au1-S1 = 173.42(3)° and for complex (**4-D**) P1A-Au1A-S1A = 173.95(3)° and P1-Au1-S1 = 171,59(2)° and for complex (**8-C**) P1-Au1-S1 = 176.78(7)° and P1A-Au1A-S1A = 175.10(5)°, as shown in Table 2 which shows some other relevant geometrical features of the complexes. The asymmetric unit reveals that the two Au(I) atoms present a nearly linear coordination. The strength of Au···Au attraction may be determined experimentally being in the range of 7 – 11 kcal mol^{-1} [47]. These findings are often associated with Au···Au bond distances in the range of 2.8 Å to 3.5 Å [47-49] which is similar or shorter than the sum of the van der Waals radii (3.40 Å) [50, 51]. The Au···Au bond in complexes (**3-C**), (**4-D**) and (**8-C**), which display moderate aurophilic interactions, present average distances of 3.110(7) Å. These results are comparable to a series of gold(I) complexes that have aurophilic interactions, such as $Au(C_5H_{10}NOS)(C_{21}H_{21}P)$ [52], $Au(3\text{-}C_4H_3S\text{–}C{\equiv}C\text{–}S)PPh_3$ [50], $(2\text{-S-pyridine-Au})_2(\mu_2\text{-}t\text{-dpen})$ [53], $(2\text{-S-pyridine-Au})_2(\mu_2\text{-dppe})$ [53] and $AuSPh(PPh_3)$ [54] with Au···Au bond distances of 3.1351(3) Å, 3.054(5) Å, 2.986(1) Å, 2.9679(2) Å and 3.145(2) Å, respectively. The coordination environment of Au(I) in complexes (**3-C**), (**4-D**) and (**8-C**) are shown in Figure 2.

Similary to complexes (**3-C**), (**4-D**) and (**8-C**), in complex (**5-E**), the central metal ion, gold(I), is coordinated to the sulfur atom of the 5-phenyl-1-(4-methoxy)-1,3,4-oxadiazole-2-thiol ligand and to a tertiary phosphine (PPh_3) in a linear geometry, with the bond angle P1-Au1-S1 = 179.01(5)°, as shown in Table 2. However, it is not possible to observe the effect of Au···Au interaction in the asymmetric unit of the compound. The coordination environment of Au(I) in complex (**5-E**) is shown in Figure 2. The P–Au–S angles for all the complexes in this work diverge from linearity which is more pronounced for complexes (**3-C**), (**4-D**) and (**8-C**). This effect may be related to the crystal packing structure or the substitution effects of groups present in the ligand. The explanation is not trivial and there is no correlation to Au···Au bond distances or bond angles, but it has been reported in the literature that gold(I) complexes, which do not present Au···Au bonds, have angles very close to 180°. For instance, $(C_6H_5)_3PAuCl$ [55] present P–Au–Cl angle of 179.63(8)°, (4-S-pyridine-Au)$_2$(μ_2-dppb) [53] exhibit P–Au–S angle of 178.32(4)° and, $[Au(C_{12}H_8N_5O_4)(PPh_3)]$ [56] show N–Au–P angle of 178.70(13)°, similar to the bond angle of 179.01(5)° found for complex (**5-E**).

The crystal structures of complexes (**3-C**, **4-D**, **5-E** and **8-C**) clearly indicates the dominance of the thiol form of the ligands (**C-E**), as evidenced by the absence of the H atom at the N1 atom and the C–S1 distance 1.709(7) Å such as in complex (**3-C**) which is intermediate between a single and a double bond (1.820 and 1.600 Å, respectively).

The crystal packing in ligand (**D**) is limited to the intermolecular hydrogen bonds formed by the oxygen atom (O4) of the DMSO molecule and nitrogen atom (N1) of the thione group, in plane ***ac*** (Figure S4). It is possible to observe weak non-classical intramolecular hydrogen bonds formed by C8-H8···O1 interactions for the ligand structure with distances Donor – Acceptor (D···A) of 2.822(3) Å. In complex (**5-E**), hydrogen bonding is restricted to the very weak non-classical intermolecular hydrogen bonds formed by C19-H19···N2 interactions between carbon atom (C19) of tertiary phosphine and ligand (**E**) with distances D···A of 3.412(7) Å. Similar weak non-classical intramolecular and intermolecular hydrogen bonds are found in the structures of complexes (**3-C**), (**4-D**) and (**8-C**) having a secundary effect for the building of the complexes structures (Fig. S5). The relevant parameters of these interactions are given in Table S2.

2.4 Anticancer activity

The anticancer activity of eight novel gold(I) complexes and two ligands was evaluated in comparison with cisplatin in two different cell lines: colon carcinoma (CT26.WT) and metastatic skin melanoma (B16F10). They were also examined for their cytotoxic properties in a non-tumor kidney cell line (BHK-21). The third cell line is a normal cell, which was used to evaluate the selectivity index, allowing comparison of the cytotoxicity of the compounds in tumor and normal cells. IC_{50} values, calculated from the cell viability dose response curves obtained after 72 h drug treatment in the MTT test, are shown in Table 3.

Insert Table 3

A major activity was found for all complexes in comparison to cisplatin and respective oxadiazole ligands and gold precursors. Free ligands were much less effective in decreasing cancer viability over these cell lines presenting IC_{50} over 50 µM in some cases. But, other ligands already showed higher cytotoxicity and selectivity comparing different cancer cells, such as ligand (**C**) in CT26.WT cells (IC_{50}< 0.10 µM and SI > 1000) and ligand (**D**) in B16F10 cells (IC_{50}< 0.26 µM and SI = 42.7). The anticancer selectivity of ligand (**C**) is impressive. Previous works suggest the influence of the fluoro substituent as electron withdrawing group improving cytotoxicity in cancer cells [57].

Even being structurally similar, some ligands presented cell-specific anticancer activity. For instance, ligand (**A**) presented equivalent anticancer activity on both tumor-derived cell lines, while ligands (**B**) and (**C**) were selectively more active against melanoma and colon carcinoma-derived cells, respectively. Ligand (**D**) has shown low IC_{50} values in both cells. The tumor cells were chosen to compose two different tumor types and assess the activity in cell lines from different embryonic origin such as epithelial and fibroblast. This was done as an effort to overcome and control any difference. Complexes (**2-B**) and (**7-B**), derived from ligand (**B**), still remaining higher cytotoxicity in B16F10 cells and became at least 30 times more active in CT26.WT after gold complexation (IC_{50} from 66µM (**B**) to 1.66µM (**2-B**) and 0.23 µM (**7-B**)). A similar pattern is observed for complexes (**3-C**) and (**8-C**), derived from ligand (**C**) in B16F10 (IC_{50} from >100µM (**C**) to 1.40 (**3-C**) and 0.43 (**8-C**). Although the ligands in the free forms showed significant activity, complexation favors the biological activity in all cases, specially for complex (**7-B**) that was about 290 and ≥ 43 times more cytotoxic than ligand (**B**) in CT26.WT and B16F10 cells, respectively.

Comparing the cytotoxicity values of the gold(I) species and their differences in the ligand structure, a better antitumoral activity was observed for complexes presenting chloride (**2-B**) and (**7-B**) and fluoride (**3-C**) and (**8-C**) as substituents (IC_{50}< 0.10μM). Another structure-activity relationship was already expected about the phosphine groups, when alkyl phosphine complexes, except (**1-A**), were slightly more active than respective aryl phosphine reported here in antileishmanial activity and in other previous antitumor reports.

Complexation also increased the cytotoxic activity in normal cell but we can notice that complexes (**2-B**) and (**3-C**) appeared to be very effective as anticancer agents against B16F10 and CT26.WT respectively, with an impressive high selectivity index (up to 70) when compared to BHK21 normal cell.

The mechanism of action is still unclear and several targets were already cited specially seleno-enzime TrxR [58]. We have previously shown the inhibition of TrxR for similar complexes and additional studies are being performed on new thiolate compounds [20].

2.5 Gold(I) complexes are highly active against Leishmania spp.

Gold(I) complexes containing phosphine and 5-phenyl-1,3,4-oxadiazole-2-thione derivatives were active against both promastigote and intracellular amastigote forms of *Leishmania* spp. (Tables 4 and S3; Fig. 3 and 4), presenting potency (IC_{50} values) ranging from 0.9 to 10.6 μM (Table 4). Unlike anticancer activity (Table 3), most ligands (**A**, **B**, **C** and **E**) were not active against the parasites except for ligand (**D**) that presented intrinsic antileishmanial activity against promastigote forms of *L. infantum* and *L. braziliensis* with potency about 30 μM. All ligands were not toxic for THP-1 macrophages. Considering the antiamastigote activity, complexes (**6-A**), (**7-B**) and (**9-D**) were the most promising candidates with IC_{50} of approximately 1 μM, presenting the highest selectivity index (SI) values (Table 4). In accordance with what was observed on anticancer activity, complex (**6-A**) was doubly selective specifically targeting both tumoral cells and *L. infantum* amastigotes (Tables 3 and 4). Although gold(I)-based compounds represents a potential niche for drug developing as alternative for leishmaniasis chemotherapy, there are few studies exploring this avenue, in which the *in vitro* antileishmanial activity reported vary from 0.2 to 54 μM [13, 59-61]. Thus, the antileishmanial activity of $Au(PEt_3)$-derivatives highlighted in the low micromolar

range are encouraging for further investigations looking for lead compounds against leishmaniasis.

Gold(I) complexes were more active against the clinically relevant intracellular amastigote forms of *L. infantum* when compared to their anti promastigote activity, being Au(PEt_3)-derivatives the most active complexes (Table 4). To investigate this point, the average of IC_{50} values from both Au(PEt_3) and Au(PPh_3)-derivatives against *Leishmania* promastigotes, amastigotes and THP-1 macrophages were obtained. Indeed, when compared to Au(PPh_3), Au(PEt_3)-derivatives presented highest antileishmanial activity towards *L. infantum* amastigotes but were also more toxic to host macrophages (Fig. 3), however, they still are selective against intracellular parasites (Table 4). A antiamastigote enhanced activity was previously observed for benzimidazole derivatives gold(I)-based complexes against *L. amazonensis, L, braziliensis*and *L. major* [60]. This was also true for *L. infantum* upon exposition to quinoline-derived gold(I) complexes [61].

As obligate intracellular parasites, *Leishmania* survives within mononuclear phagocyte system cells in mammalian hosts causing leishmaniasis [11]. Thus, intramacrophagic amastigotes obtained by *in vitro* experimental infection, mimic the natural environment for antileishmanial drug prospection. Indeed, active compounds identified by drug screening assays on intracellular *Leishmania* can highlight and suggest the involvement of host cell-dependent mechanisms related to parasite survival [62]. Here we demonstrate that Au(PEt_3)-derivatives presented increased antiamastigote activity offering an evidence for the importance of host cell pathways on drug activity and corroborating the relevance to the use of intracellular parasite for drug screening purposes. Since drug action is initially dependent on the uptake/transport through cell membrane, to reach intracellular amastigotes, active compounds must cross the macrophage and phagolysosome membranes. Amastigote-selective gold(I)-based complexes could provide insights to infer about host-dependent drug transport pathways [63].

Insert Table 4

Insert Fig. 3

Drug susceptibility in *Leishmania* parasites is species-specific or can vary even among strains of the same species as a result of distinct metabolisms [63, 64]. In this study we shown that *L. braziliensis* was less sensitive to Au(PEt_3)-derivatives when

compared to *L. infantum* and *L. guyanensis*, presenting mean of IC_{50} values of 7.3, 4.5 and 3.5 μM, respectively (Table 4 and S3; Fig. 3). This fact can provide clues about the mode of action of antileishmanial gold(I)-based complexes focused on species-specific biochemical properties.

Although $Au(PEt_3)Cl$ and $Au(PPh_3)Cl$ precursors were toxic to THP-1 macrophages and active themselves against *Leishmania*, their use as antileishmanial drugs can be justified by the reduced cytotoxicity on host cells upon 5-phenyl-1,3,4-oxadiazole-2-thione complexation. For $Au(PPh_3)$-derivatives the average IC_{50} was 10.5 μM, twice less toxic when compared to precursor alone (Table 4). Here, we found that $Au(PEt_3)Cl$ exhibited inherent antileishmanial activity with IC_{50} of 1.94 and 2.8 μM against *L. infantum*and *L. braziliensis*, respectively (Table 4). In contrast, Ilari and cols. (2012) observed a lower antileishmanial activity against *L. infantum* and *L. major* presented by $Au(PEt_3)Cl$ with higher IC_{50} values of 16.6 and 17.5 μM, respectively [13]. This difference can be explained by the fact that, in drug susceptibility assays they used Schneider's medium, a very nutrient rich cell culture medium that could interfere by drug binding to its constituents or improving cell growth fitness, masking the real antileishmanial activity. As mentioned, $Au(PEt_3)$-derivatives exhibited most promising antileishmanial activity than $Au(PPh_3)$ ones. This is in accordance with Sharlow and cols. (2013), who shown that chloro(triethylphosphine)gold(I) precursor presented highest antileishmanial effect against *L. major* and *L. amazonensis* when compared to chloro(triphenylphosphine)gold(I) [18].

2.6 Gold(I) complexes with 5-phenyl-1,3,4-oxadiazole-2-thione and triethylphosphine as ligands present cross-resistance to antimony in Leishmania

Drug resistant *Leishmania* can be applied as a tool for understanding parasite biochemical pathways involved in drug resistance, mechanisms of action and for drug screening purposes [65-68]. To investigate whether antileishmanial activity displayed by gold(I) complexes would be affected by a drug-resistant background in *Leishmania*, we performed growth inhibition assays using the most active $Au(PEt_3)$-derivatives against antimony-resistant and -sensitive *L. guyanensis* promastigotes. Surprisingly, gold(I) 5-phenyl-1,3,4-oxadiazole-2-thione triethylphosphine derivatives were 1.5 to 2.2-fold less active in antimony-resistant *L. guyanensis* background, thus presenting cross-resistance to antimony (Fig. 4 and Table S3).

Insert Fig. 4

This is suggestive that gold(I) complexes could share similar targets or their mechanisms of action would involve parasite biochemical pathways related to antimony action/resistance. Trivalent antimony (SbIII) – the active reduced form from SbV-based drugs – can act disrupting the redox homeostasis by inducing thiol efflux or inhibiting trypanothione reductase (responsible for recycling trypanothione, the major intracellular antioxidant dithiol), promoting oxygen reactive species accumulation, triggering cell death by oxidative stress [69]. Auranofin, a gold(I)-based compound is also able to inhibit trypanothione reductase (TryR) of *Leishmania* parasites [13]. Known by its clinical application to treat rheumatoid arthritis [70] with recognized antitumor [15], antiparasitic [19, 71] and antimicrobial activity [72], auranofin is a selenoprotein antagonist inhibiting thioredoxin reductase in cancer cells by binding selenium residues [23]. Unlike in mammals, auranofin-mediated redox homeostasis disruption in *Leishmania* is not due to selenoproteins [73] but involves TryR inhibition through binding to cysteine residues instead [13]. Triethylphosphine gold(I) complexes are potent TryR inhibitors showing IC_{50} of 1 μM (L. Tunes and R. Monte-Neto, manuscript in preparation), more active than the positive control clomipramine – a strong inhibitor of TryR with IC_{50} values of 3.4 and 11.1 μM against TryR from *Trypanosoma cruzi* and *T. brucei*, respectively [74] – and gold(III)-based complexes [14].

It is worthy of note that free $Au(PEt_3)Cl$ precursor or a gold(I) 5-phenyl-1,3,4-oxadiazole-2-thione triethylphosphine analog – where phenyl group was replaced by adamantly [20] presented no cross-resistance to antimony (Fig. 4 and Table S3). The differential sensitivity profile provides functional evidences, based on structure activity relationship, indicating that 5-phenyl and 5-adamantyl substituents interferes with gold(I) pharmacophore dynamics in Sb-resistant *L. guyanensis* parasites compared to wild-type background (Fig. 4). A wide variety of biochemical and biophysical changes is observed in drug-resistant *Leishmania* parasites including increased membrane fluidity [75, 76]. Thus, it is tempting to speculate that triethylphosphine gold(I) complexes lipophilicity would interfere with their transport across membranes altering the drug target(s) achievement, a point that needs to be further investigated. In general, the presence of *para*-phenyl ligands chloride, fluoro, nitro and methoxy groups interfered with the global antileishmanial activity displayed by their gold(I) triethylphosphine derivative, reducing its action against promastigote and amastigote

Leishmania parasistes (Table 4 and S3). However, they do not altered (Cl and F) or slightly decreased (NO_2 and OCH_3) the resistance index when assayed on Sb-resistant *L. guyanensis* (Fig. 4). These observations reinforce the importance of tryethylphosphine gold(I) complexes not only as promising antileishmanial agents but also as chemical tools to better understand cellular and molecular mechanisms in drug resistant parasites. Gold(I) complexes can be applied for drug target elucidation and for the identification of parasite's essential biochemical pathways involved in their mechanisms of action, which is extremely relevant for drug specificity approaches on drug discovery studies. Based on structucture optimisation, gold(I) complexes can be designed to overcome drug resistance in *Leishamania* parasites.

These promising results prompted us to evaluate the antileishmanial activity of novel gold(I) oxadiazole phosphine derivatives. We were also inspired by the fact that auranofin (Ridaura®) – a gold(I) triethylphosphine thiosugar drug with known pharmacokinetics and pharmacodynamics against leishmaniasis – is able to inhibit TryR, a crucial enzyme for redox homeostasis in trypanosomatid protozoa including *Leishmania* [13, 18]. All gold(I) oxadiazole phosphine derivatives tested here were active *in vitro* against *Leishmania* parasites, with special emphasis on triethylphosphine derivatives. They were not only promising drug candidates to be investigated as their efficacy against leishmaniasis *in vivo*, but can also be applied as chemical tools to understand mechanisms of action of gold-containing drugs in *Leishmania* parasites. Based on rational drug design approaches, use of gold(I)-containing drugs represents a plausible way for the development of new therapeutic strategies against leishmaniasis. Chrysotherapy (treatment of diseases based on the administration of gold compounds) must be further investigated as a *golden alternative* for leishmaniasis chemotherapy.

3. Conclusions

A novel series of gold(I) complexes containing phosphine and 5-phenyl-1,3,4-oxadiazole-2-thione derivatives as ligands were synthesized, characterized and evaluated for their *in vitro* activity against tumoral cell lines and *Leishmania* spp. Gold(I) complexes were successful synthesized in good yields (mostly 62 to 84%). The crystal structures of complexes (**3-C**, **4-D**, **5-E** and **8-C**) showed that S-atom of thione group is coordinated to the metal in all cases and the dominance of the thiol form of the ligands.

Gold(I) complexes studied here were highly active against murine melanoma B16F10 and colon cancer CT26.WT cell lines with potency on nanomolar range. Most compounds were more active than the reference anticancer drug cisplatin against B16F10 and CT26.WT cell lines with high selectivity indexes. Upon complexation compound (**7-B**) was about 300 times more active than the free ligand on CT26.WT cell line. Ligands also increased gold(I) chloride precursors anticancer activity being the resulting complexes approximately 30 folds more selective against tumoral cells. Complexation also reduces the cytotoxicity on human monocyte-derived THP-1 macrophages. All phosphine oxadiazole-containing gold(I) complexes were active against *Leishmania* spp. Triethylphosphine gold(I) derivatives were the most promising anticancer and antileishmanial leads, being compound (**6-A**) selective to tumoral cells and *L. infantum* intracellular amastigotes, the clinically relevant form of the parasite. Antimony-resistant *L. guyanensis* were cross-resistant when treated with 5-phenyl-1,3,4-oxadiazole-2-thione gold(I) derivatives, but they were still susceptible to precursor $Au(PEt_3)Cl$, showing that gold(I) complexes are not only promising antileishmanial candidates but can be also used as tools helping to elucidate molecular mechanisms of drug action and drug resistance in *Leishmania* parasites. The findings here reveal the remarkable ability of phosphine oxadiazole-containing gold(I) complexes to selectively inhibit cancer cell proliferation and the growth of *Leishmania* parasites *in vitro*. This first report of phosphine oxadiazole-containing gold(I) as potential anticancer and antileishmanial agents encourages the efforts on metallodrug prospection to treat cancer and leishmaniasis. Due to the good yields on synthesis and to noteworthy antiproliferative effect on cancer cells and antileishmanial properties, the tested gold(I) complexes are suitable for further *in vivo* efficacy studies against experimental leishmaniasis and murine tumor models.

4. Experimental section

4.1 Chemistry

All reagents and solvents were reagent grade and were used without prior purification. The progress of all reactions was monitored by thin-layer chromatography which was performed on 2 x 6 cm aluminium sheets precoated with silica gel 60 (HF-254, Merck) to a thickness of 0.25 mm. Infrared (IR) spectra were recorded on a Bomem FTIR MB-102 spectrometer in the region of 4000-500 cm^{-1} as a KBr pellet,

with 4 cm^{-1} of spectral resolution, and average of 64 scans. Only significant peaks were recorded. ^{1}H NMR (300 MHz) and ^{13}C NMR (75 MHz) spectra were recorded as solutions in $CDCl_3$ and DMSO-d_6 on a Bruker spectrometer. The chemical shifts were expressed as δ (in ppm) with respect to a standard internal TMS reference (^{1}H NMR). Raman spectra were obtained using a Bruker RFS 100 FT-Raman instrument equipped with a germanium detector refrigerated by liquid nitrogen, with excitation at 1064 nm from a Nd: YAG laser, power between 103 mW for sample in solid phase, in the range between 4000 and 50 cm^{-1}, and with a spectral resolution of 4 cm^{-1}, and an average of 500 scans. The high-resolution mass spectra were recorded on a Micromass LCT spectrometer, with electrospray ionization, at the Institut de Chimie des Substances Naturelles at Gif-sur-Yvette, France. Diffraction data for single crystals of $C_8H_5N_3O_3S$ (**D**), $C_{26}H_{19}N_2OFPSAu$ (**3-C**), $C_{26}H_{19}N_3O_3PSAu$ (**4-D**), $C_{27}H_{22}N_2O_2PSAu$ (**5-E**) and $C_{14}H_{19}N_2OPSAuF$ (**8-C**) were collected using a Oxford GEMINI A Ultra diffractometer with Mo K α (λ = 0.71073 Å) and temperature of 120 K or 298 K. Data collection, reduction and cell refinement were carried out by CRYSALIS RED, Oxford diffraction Ltd – Version 1.171.32.38 software [77]. The structures were solved using SHELXS-97 [78] and refined using SHELXL-2013 [79]. An empirical isotropic extinction parameter x was refined according to the method described by Larson [80]. A Multiscan absorption correction was applied [81]. The structures were drawn by ORTEP-3 for Windows [82] and MERCURY programs [83].

4.2 Synthesis of ligands

We have recently published the synthesis of ligand (**A**) [37]. Ligands (**B**-**E**) were prepared from 4-chlorobenzoic, 4-fluorobenzoic, 4-nitrobenzoic and 4-methoxybenzoic acids in three steps as previously described [32, 35, 84, 85]. The characterization data of the ligands are described in supplementary material section.

4.3 Synthesis of Gold(I) complexes

Precursors $Au(PEt_3)Cl$ and $Au(PPh_3)Cl$ were respectively, purchased from Sigma-Aldrich and synthesized from $K[AuCl_4]$ according to the Baenziger and cols (1976) [86]. Synthesis of complexes (**1-A**) and (**6-A**) was performed as previously published [37].

Complexes **2-B**, **3-C**, **4-D**, **5-E** and **7-B**, **8-C**, **9-D**, **10-E** were prepared according to the following procedure: to a solution of $Au(PPh_3)Cl$ (0.198 g, 0.4 mmol)

or Au(PEt_3)Cl (0.140 g, 0.4 mmol) in dichloromethane (3 mL), ligands (**B**-**E**) (0.4 mmol) were dissolved in acetone (3 mL) and slowly added during 3 h. After stirring for 9 h at room temperature in the dark, solvent was removed under reduced pressure to furnish a white residue that was purified by preparative chromatography (eluent: dichloromethane) to give the desired compounds (**2**-**B**, **3**-**C**, **4**-**D**, **5**-**E**) and (**7**-**B**, **8**-**C**, **9**-**D**, **10**-**E**) in 64%, 69%, 62%, 63%, 67%, 84%, 51% and 65% yields, respectively (Scheme 1).

Insert Scheme 1

Insert Scheme 2

*4.3.1 [5-(4-Chlorophenyl)-1,3,4-oxadiazole-2-thione](triphenylphosfine)gold(I)***(2-B)**
yield, (64%) as a white solid, m.p. 181-182ºC. IR ν_{max} KBr (cm^{-1}): 3054; 1481; 1068, 710; Raman ν_{max} (cm^{-1}): 3059; 1547; 744; ^{1}H NMR (300 MHz, DMSO-d_6) δ: 7.59-7.66 (m, 15H, $ArPPh_3$); 8.07 (d, 2H, $J_{7-8} = J_{11-10}$ = 9.0 Hz, H7, H11); 8.34 (d, 2H, $J_{8-7} = J_{10-11}$ = 9.0 Hz, H.8, H.10); ^{13}C NMR (75 MHz, DMSO-d_6) δ: 124.5 (C8, C10); 126.9 (C7, C11); 128.3 (d, C1', $J_{1'-P}$= 58.7 Hz); 129.1 (C6); 129.7 (d, C3', C5', $J_{3'-P} = J_{5'-P}$ = 11.5 Hz); 132.3 (C4'); 133.9 (d, C2', C6', $J_{2'-P} = J_{6'-P}$ = 14.0 Hz); 148.6 (C9); 162.6 (C5); 169.9 (C2).

*4.3.2 [5-(4-Fluorophenyl)-1,3,4-oxadiazole-2-thione](triphenylphosfine)gold(I)***(3-C)**
yield, (69%) as a white solid, m.p. 159-160 ºC. IR ν_{max} KBr (cm^{-1}): 3056; 1499; 1062; 713; Raman ν_{max} (cm^{-1}): 3064; 1560; 725; ^{1}H NMR (300 MHz, DMSO-d_6) δ: 7.38 (t, 2H, $J_{8-7} = J_{8-F}$ = 8.7 Hz, H8, H10); 7.57-7.61 (m,15H, Ar-PPh_3); 7.80 (dd, 2H, J_{7-8} = 8.7 HZ, J_{7-F} = 5.4 Hz, H7, H11); ^{13}C NMR (75 MHz, DMSO-d_6) δ: 116.4 (d, C8, C10, $J_{8-F} = J_{10-F}$ = 22.4 Hz); 120.4 (C6); 128.3 (d, C7, C11, $J_{7-F} = J_{11-F}$ = 9.0 Hz); 128.4 (d, C1', $J_{1'-P}$= 58.1 Hz); 129.6 (d, C3', C5', $J_{3'-P} = J_{5'-P}$ = 11.4 Hz); 132.2 (C4'); 133.8 (d, C2', C6', $J_{2'-P} = J_{6'-P}$ = 13.9 Hz); 163.0 (C5); 163.6 (d, C9, J_{9-F} = 247.9 Hz); 168.2 (C2).

4.3.3 [5-(4-Nitrophenyl)-1,3,4-oxadiazole-2-thione](triphenylphosfine)gold(I) **(4-D)**
yield, (62%) as a yellow solid, m.p. 223 ºC. IR ν_{max} KBr (cm^{-1}): 3029; 1555; 1515; 1339; 1068; 707; Raman ν_{max} (cm^{-1}): 3057; 1553; 1341; 694; ^{1}H NMR (300 MHz, DMSO-d_6) δ: 7.59-7.66 (m, 15H, $ArPPh_3$); 8.07 (d, 2H, $J_{7-8} = J_{11-10}$ = 9.0 Hz, H7, H11);

8.34 (d, 2H, $J_{8\text{-}7}$ = $J_{10\text{-}11}$ = 9.0 Hz, H8, H10); ^{13}C NMR (75 MHz, DMSO-d_6) δ: 124.5 (C8, C10); 126.9 (C7, C11); 128.3 (d, C1', $J_{1'\text{-}P}$= 58.7 Hz); 129.1 (C6); 129.7 (d, C3', C5', $J_{3'\text{-}P}$ = $J_{5'\text{-}P}$ = 11.5 Hz); 132.3 (C4'); 133.9 (d, C2', C6', $J_{2'\text{-}P}$= $J_{6'\text{-}P}$ = 14.0 Hz); 148.6 (C9); 162.6 (C5); 169.9 (C2).

*4.3.4 [5-(4-Methoxyphenyl)-1,3,4-oxadiazole-2-thione](triphenylphosfine)gold(I)***(5-E)** yield, (63%) as a white solid, m.p. 178-181 ºC. IR ν_{max} KBr (cm^{-1}): 3055; 1499; 1065; 710; Raman ν_{max} (cm^{-1}): 3059; 1560; 629; ^{1}H NMR (300 MHz, DMSO-d_6) δ: 3.83 (S, 3H, OCH_3); 7.07 (d, 2H, $J_{8\text{-}7}$ = $J_{10\text{-}11}$ = 8.7 Hz, H8, H10); 7.57-7.66 (m, 15H, $ArPPh_3$); 7.78 (d, 2H, $J_{7\text{-}8}$ = $J_{11\text{-}10}$ = 8.7 Hz, H7, H11). ^{13}C NMR (75 MHz, DMSO-d_6) δ: 55.9 (OCH_3); 115.2 (C8, C10); 116.5 (C6); 128.1 (C7, C11); 128.9 (d, C1', $J_{1'\text{-}P}$= 58.4 Hz); 130.1 (d, C3', C5', $J_{3'\text{-}P}$ = $J_{5'\text{-}P}$ = 11.5 Hz); 132.7 (C4'); 134.3 (d, C2', C6', $J_{2'\text{-}P}$= $J_{6'\text{-}P}$ = 14.0 Hz); 162.1 (C9); 163.9 (C5); 168.7 (C2); HRMS(ESI): m/z calculated for [$C_{27}H_{22}N_2O_2PSAu$] $[M+H]^+$ calc.(667.0883) found (667.0870).

4.3.5 [5-(4-Chlorophenyl)-1,3,4-oxadiazole-2-thione](triethylphosphine)gold(I) **(7-B)** yield, (67%) as a white solid, m.p. 127-129 ºC. IR ν_{max} KBr (cm^{-1}): 3070; 1478; 1070; 689; Raman ν_{max} (cm^{-1}): 3076; 1553; 750; ^{1}H NMR (300 MHz, DMSO-d_6) δ: 1.09-1.21 (m, 9H, CH_3); 1.92-2.02 (m, 6H, CH_2); 7.60 (d, 2H, $J_{8\text{-}7}$ = $J_{10\text{-}11}$ = 8.4 Hz, H8, H10); 7.85 (d, 2H, $J_{7\text{-}8}$ = $J_{11\text{-}10}$ = 8.4 Hz, H7, H11); ^{13}C NMR (75 MHz, DMSO-d_6) δ: 9.1 (CH_3); 16.9 (d, CH_2, $J_{CH2,P}$ = 34.6 Hz); 122.6 (C6); 127.6 (C7, C11); 126.5 (C8, C10); 136.0 (C9); 162.7 (C5); 169.7 (C2); HRMS(ESI): m/z calculated for [$C_{14}H_{19}N_2OPSAuCl$] $[M+H]^+$ calc.(527.0388) found (527.0378).

4.3.6 [5-(4-Fluorophenyl)-1,3,4-oxadiazole-2-thione](triethylphosphine)gold(I) **(8-C)** yield, (84%) as a white solid, m.p. 65-66 ºC. IR ν_{max} KBr (cm^{-1}): 3071; 2962; 1498; 1065; 693; Raman ν_{max} (cm^{-1}): 3083; 2920; 1565; 706; ^{1}H NMR (300 MHz, DMSO-d_6) δ: 1.10-1.21 (m, 9H, CH_3); 1.92-2.04 (m, 6H, CH_2); 7.40 (t, 2H, $J_{8\text{-}7}$ = $J_{8\text{-}F}$ = 8.7 Hz, H8, H10); 7.92 (dd, 2H, $J_{7\text{-}8}$ = 8.7 HZ, $J_{7\text{-}F}$ = 5.4 Hz, H7, H11);^{13}C NMR (75 MHz, DMSO-d_6) δ: 9.1 (CH_3); 16.9 (d, CH_2, $J_{CH2,P}$ = 34.6 Hz); 116.6 (d, C8, C10, $J_{8\text{-}F}$ = $J_{10\text{-}F}$ = 22.4 Hz); 120.4 (C6); 128.4 (d, C7, C11, $J_{7\text{-}F}$ = $J_{11\text{-}F}$ = 9.0 Hz); 162.7 (C5); 163.4 (d, C9, $J_{9\text{-}F}$ = 247.9 Hz); 168.2 (C2); HRMS(ESI): m/z calculated for [$C_{14}H_{19}N_2OPSAuF$] $[M+H]^+$ calc.(511.0684) found (511.0665).

*4.3.7 [5-(4-Nitrophenyl)-1,3,4-oxadiazole-2-thione](triethylphosphine)gold(I)***(9-D)** yield, (51%) as a yellow solid, m.p. 180-181 ºC. IR ν_{max} KBr (cm^{-1}): 3066; 2964; 1552; 1519, 1345; 1070; 706; Raman ν_{max} (cm^{-1}): 3082; 2947; 1554; 1343; 758; ^{1}H NMR (300 MHz, DMSO-d_6) δ: 1.11-1.23 (m, 9H, CH_3); 1.94-2.06 (m, 6H, CH_2); 8.10 (d, 2H, $J_{7-8} = J_{11-10}$ = 9.0 Hz, H7, H11); 8.34 (d, 2H, $J_{8-7} = J_{10-11}$ = 9.0 Hz, H8, H10); ^{13}C NMR (75 MHz, DMSO-d_6) δ: 9.0 (CH_3); 16.9 (d, CH_2, $J_{CH2,P}$ = 34.6 Hz); 124.6 (C8, C10); 126.9 (C7, C11); 129.2 (C6); 148.6 (C9); 162.3 (C5); 170.4 (C2); HRMS(ESI): m/z calculated for $[C_{14}H_{19}N_3O_3PSAu]$ $[M+H]^+$calc.(538.0629) (found 538.0615).

*4.3.8 [5-(4-Methoxyphenyl)-1,3,4-oxadiazole-2-thione](triethylphosphine)gold(I)***(10-E)** yield, (65%) as a white solid, m.p. 103-104 ºC. IR ν_{max} KBr (cm^{-1}): 3069; 2967; 1499; 1070; 703; Raman ν_{max} (cm^{-1}): 3078; 2920; 1565; 646; ^{1}H NMR (300 MHz, DMSO-d_6) δ: 1.10-1.21 (m, 9H, CH_3); 1.92-2.03 (m, 6H, CH_2); 3.82 (S, 3H, OCH_3); 7.10 (d, 2H, $J_{8-7} = J_{10-11}$ = 8.7 Hz, H8, H10); 7.79 (d, 2H, $J_{7-8} = J_{11-10}$ = 8.7 Hz, H7, H11); ^{13}C NMR (75 MHz, DMSO-d_6) δ: 9.1 (CH_3); 16.9 (d, CH_2, $J_{CH2,P}$ = 34.6 Hz); 55.4 (OCH_3); 114.7 (C8, C10); 116.2 (C6); 127.5 (C7, C11); 161.5 (C9); 163.4 (C5); 168.2 (C2); HRMS(ESI): m/z calculated for $[C_{15}H_{23}N_2O_2PSAu]$ $[M+H]^+$calc. (523.0883) found (523.0869).

4.4 Cytotoxicity and antitumoral activity

In vitro cytotoxicity and antitumoral activity were evaluated by quantifying the ability of living cells to reduce the yellow dye 3-(4,5-dimethyl-2-thiazolyl)-2,5-diphenyl-2H-tetrazolium bromide (MTT) to a purple formazan product [87]. Anticancer activity was investigated against tumor derived cell lines CT26.WT (colon cancer cells) and B16-F10 (mouse metastatic skin melanoma), while cytotoxicity (cell viability) was evaluated on human monocyte-derived THP-1 macrophages and non-tumor Baby Hamster Kidney (BHK-21) cell lines. All cell lines were propagated in RPMI 1640 culture medium pH 7.4, supplemented with 10% heat-inactivated Fetal Bovine Serum (FBS), Hepes (4 mM), $NaHCO_3$ (14 mM), ampicillin (0.27 mM), and streptomycin (0.06 mM). Adherent cells were harvested by trypsinization and seeded in 96-well tissue culture plates(1 x 10^3 viable cells/well in 100 µL) and incubated at 37 ºC in a humidified atmosphere of 5% CO_2 for 24 h. For THP-1 macrophages differentiation, 5 x

10^5 precursors monocytes/well were seeded in 96-well plates treated with 20 ng/mL phorbol myristate acetate [43] and incubated 48 h at 37 ºC in 5% CO_2 humid atmosphere. Stock solutions of gold(I) complexes were prepared in DMSO and serially diluted in RPMI 1640 medium (<1% DMSO). After 72 h of drug exposure at 37 ºC/5% CO_2, cells were incubated with MTT (10mM in water solution – 10 µL/well) for 4 h at 37 ºC and 5% CO_2. MTT is metabolized by viable cells resulting in a purple product that, after being solubilized in 100 µL of DMSO, can be quantified through colorimetric assay using a plate reader (absorbance at 570 nm). Negative control was performed considering untreated cells in RPMI 1640. Cisplatin and amphotericin B (AmB) were purchased from Sigma-Aldrich (St. Louis, MO, USA) and Miltefosine [88] obtained from Cayman Chemical (Ann Arbor, MI, USA). Cisplatin was used as reference anticancer agent, while AmB and MIL as antileishmanial drugs.

4.5 In vitro antileishmanial assays

4.5.1 Parasite strains

L. (*Leishmania*) *infantum* (strain MHOM/BL/1967/ITMAP263); *L.* (*Viannia*) *braziliensis* (strain MHOM/BR/1975/M2904) and *L.* (*Viannia*) *guyanensis* (strains MHOM/BR/1975/M4147 sensitive, wild-type WT and antimony resistant, Sb^{III}650.4) promastigotes were maintained in minimum essential culture medium (α-MEM) (Gibco, Invitrogen NY, USA) supplemented with 10% (v/v) heat inactivated FBS (Cultilab, Campinas, SP, Brazil), 100 mg/mL kanamycin, 50 mg/mL ampicillin, 2 mM L-glutamine, 5 mg/mL hemin, 5 mM biopterin (Sigma-Aldrich, St Louis, USA), at pH 7.0 and incubated at 25 °C. *L.* (*V.*) *guyanensis* was selected for SbIII resistance (LgSbR) through stepwise drug selection as previously described [65]. This resistant line is > 18.6-fold more resistant to SbIII than its parental WT counterpart. Briefly, *L. guyanensis* promastigotes were seeded in 25 cm^2 flasks containing 5 mL of α-MEM in the presence of increasing concentration of Sb^{III} from 40 up to 650 µM.

4.5.2 Antipromastigote activity

Log-phase *L. infantum* and *L. braziliensis* promastigotes (1×10^6 parasites/mL) were seeded in 24-wells cell culture plates containig 1.5 mL of α-MEM and incubated under shaking at 25 °C during 72 h in the presence of several concentrations of gold(I) complexes. Controls were performed using cultures in the presence of amphotericin B

and miltefosine. Non-treated parasites were established for growth comparison. Stock solutions of gold(I) complexes were dissolved in DMSO and diluted in α-MEM cell culture medium to obtain the range of tested concentrations. The final DMSO concentration did not exceed 1%, which is known to be nontoxic to *Leishmania* parasites [89]. For drug susceptibility assay, *Leishmania* growth curves were constructed by measuring absorbance at 600 nm [90]. The antileishmanial activity is expressed as IC_{50}/72 h, which is the concentration that reduces cell growth by 50% compared to untreated control (growth inhibition). All experiments were done at least three times as independent experiments performed in triplicate. Gold(I) complexes (**6-A**, **7-B**, **8-C**, **9-D** and **10-E**) were also evaluated *in vitro* for their activity against both Sb^{III}-sensitive and -resistant *L. guyanensis* parasites.

4.5.3 Antiamastigote activity

For this assay *L. infantum* parasites were transfected with an episomal vector containing the firefly luciferase as reporter gene (pSP72αHYGαLUC1.2) as previously described [91]. Human monocyte-derived macrophage cell line THP-1 (1.5 x 10^5 cells/well) was maintained in RPMI 1640 medium supplemented with 10% FBS and differentiated in presence of 20 ng/mL PMA, incubated at 37 °C in a 5% CO_2 containing humid atmosphere for 3 days. Cells were washed with pre-warmed RPMI medium and subsequently infected with *L.infantum* LUC promastigotes (1.5 x 10^6 parasites/well) at a parasite/macrophage ratio of 10:1 for 3 h in a blank 96-well tissue culture plate. Non-internalized parasites were removed by three washes with pre-warmed HEPES/NaCl buffer (20 mM HEPES, 0.15 M NaCl, 10 mM glucose, pH 7.2). Experimentally infected macrophages were then exposed to different concentrations of gold(I)-derived complexes and incubated during 72 h at 37 °C in a 5% CO_2 containing humid atmosphere. After 3 days incubation RPMI was aspirated and the luciferase activity was assessed by adding 20 μL of reconstituted One-Glo™ Luciferase Assay System solution as enzyme substrate, following manufacturer's instructions (Promega, Madison, WI, USA). Luciferase activity was measured by luminescence detection in a luminometer SpectraMax M5 (Molecular Devices, Sunnyvale, CA, USA) using 1 second integration/well. Non-infected THP-1 macrophages were used as signal background while non-treated infected THP-1 was used as control for growth comparison. AmB and MIL were used as positive control.

4.6 Statistical analyses

IC_{50} and CC_{50} values were calculated based on concentration-response curves applying a sigmoidal dose-response equation with variable slope carried out using the software GraphPad Prism version 6.0 (GraphPadSoftware Inc., San Diego, CA, USA). When applied, data were analyzed by Student's t test or analysis of variance (ANOVA) followed by correction performed using Bonferroni'smultiple comparison test. A p value < 0.05 was considered statistically significant.

Acknowledgments

This work is a collaboration research project of members of the Rede Mineira de Química (RQ-MG) supported by FAPEMIG (Project: REDE-113/10). RLMN holds a young talent investigator fellowship from National Council for Scientific and technological Development (CNPq) (314024/2013-1; 401936/2013-9). LGT is a recipient of a doctoral studentship from Coordination for the Improvement of Higher Education Personnel (CAPES). HS is the holder of FAPEMIG (APQ-01648-14) and CNPq (455548/2014-5) grants that supported this study. The authors thank FAPEMIG, CAPES and CNPq for financial support.

Appendix A. Supplementary material

References

[1] M.R. Stratton, P.J. Campbell, P.A. Futreal, The cancer genome, Nature, 458 (2009) 719-724.
[2] J. Alvar, I.D. Velez, C. Bern, M. Herrero, P. Desjeux, J. Cano, J. Jannin, M. den Boer, W.H.O.L.C. Team, Leishmaniasis worldwide and global estimates of its incidence, PLoS One, 7 (2012) e35671.
[3] M. May, Statistics: Attacking an epidemic, Nature, 509 (2014) S50-51.
[4] J.M. Ubeda, F. Raymond, A. Mukherjee, M. Plourde, H. Gingras, G. Roy, A. Lapointe, P. Leprohon, B. Papadopoulou, J. Corbeil, M. Ouellette, Genome-wide stochastic adaptive DNA amplification at direct and inverted DNA repeats in the parasite Leishmania, PLoS Biol, 12 (2014) e1001868.
[5] T.P. Dorlo, M. Balasegaram, J.H. Beijnen, P.J. de Vries, Miltefosine: a review of its pharmacology and therapeutic efficacy in the treatment of leishmaniasis, J Antimicrob Chemother, 67 (2012) 2576-2597.
[6] A.B. Caballero, A. Rodriguez-Dieguez, M. Quiros, J.M. Salas, O. Huertas, I. Ramirez-Macias, F. Olmo, C. Marin, G. Chaves-Lemaur, R. Gutierrez-Sanchez, M. Sanchez-Moreno, Triazolopyrimidine compounds containing first-row transition metals and their activity against the neglected infectious Chagas disease and leishmaniasis, Eur J Med Chem, 85 (2014) 526-534.
[7] M.K. Rauf, S. Yaseen, A. Badshah, S. Zaib, R. Arshad, D. Imtiaz Ud, M.N. Tahir, J. Iqbal, Synthesis, characterization and urease inhibition, in vitro anticancer and antileishmanial

studies of Ni(II) complexes with N,N,N'-trisubstituted thioureas, J Biol Inorg Chem, 20 (2015) 541-554.
[8] S. Yaseen, M.K. Rauf, S. Zaib, A. Badshah, M.N. Tahir, M.I. Ali, D. Imtiaz ud, M. Shahid, J. Iqbal, Synthesis, characterization and urease inhibition, in vitro anticancer and antileishmanial studies of Co(III) complexes with N,N,N'-trisubstituted acylthioureas, Inorganica Chimica Acta, 443 (2016) 69-77.
[9] S. Kaur, H. Sachdeva, S. Dhuria, M. Sharma, T. Kaur, Antileishmanial effect of cisplatin against murine visceral leishmaniasis, Parasitol Int, 59 (2010) 62-69.
[10] M. Navarro, C. Hernandez, I. Colmenares, P. Hernandez, M. Fernandez, A. Sierraalta, E. Marchan, Synthesis and characterization of [Au(dppz)2]Cl3. DNA interaction studies and biological activity against Leishmania (L) mexicana, J Inorg Biochem, 101 (2007) 111-116.
[11] R.J. Pulvertaft, G.F. Hoyle, Stages in the life-cycle of Leishmania donovani, Trans R Soc Trop Med Hyg, 54 (1960) 191-196.
[12] S.P. Fricker, R.M. Mosi, B.R. Cameron, I. Baird, Y. Zhu, V. Anastassov, J. Cox, P.S. Doyle, E. Hansell, G. Lau, J. Langille, M. Olsen, L. Qin, R. Skerlj, R.S. Wong, Z. Santucci, J.H. McKerrow, Metal compounds for the treatment of parasitic diseases, J Inorg Biochem, 102 (2008) 1839-1845.
[13] A. Ilari, P. Baiocco, L. Messori, A. Fiorillo, A. Boffi, M. Gramiccia, T. Di Muccio, G. Colotti, A gold-containing drug against parasitic polyamine metabolism: the X-ray structure of trypanothione reductase from Leishmania infantum in complex with auranofin reveals a dual mechanism of enzyme inhibition, Amino Acids, 42 (2012) 803-811.
[14] G. Colotti, A. Ilari, A. Fiorillo, P. Baiocco, M.A. Cinellu, L. Maiore, F. Scaletti, C. Gabbiani, L. Messori, Metal-based compounds as prospective antileishmanial agents: inhibition of trypanothione reductase by selected gold complexes, ChemMedChem, 8 (2013) 1634-1637.
[15] C.K. Mirabelli, R.K. Johnson, C.M. Sung, L. Faucette, K. Muirhead, S.T. Crooke, Evaluation of the in vivo antitumor activity and in vitro cytotoxic properties of auranofin, a coordinated gold compound, in murine tumor models, Cancer Res, 45 (1985) 32-39.
[16] M. Altaf, M. Monim-ul-Mehboob, A.A.A. Seliman, M. Sohail, M.I.M. Wazeer, A.A. Isab, L. Li, V. Dhuna, G. Bhatia, K. Dhuna, Synthesis, characterization and anticancer activity of gold(I) complexes that contain tri-tert-butylphosphine and dialkyl dithiocarbamate ligands, European Journal of Medicinal Chemistry, 95 (2015) 464-472.
[17] I. Ott, On the medicinal chemistry of gold complexes as anticancer drugs, Coordination Chemistry Reviews, 253 (2009) 1670-1681.
[18] E.R. Sharlow, S. Leimgruber, S. Murray, A. Lira, R.J. Sciotti, M. Hickman, T. Hudson, S. Leed, D. Caridha, A.M. Barrios, D. Close, M. Grogl, J.S. Lazo, Auranofin is an apoptosis-simulating agent with in vitro and in vivo anti-leishmanial activity, ACS Chem Biol, 9 (2014) 663-672.
[19] A. Caroli, S. Simeoni, R. Lepore, A. Tramontano, A. Via, Investigation of a potential mechanism for the inhibition of SmTGR by Auranofin and its implications for Plasmodium falciparum inhibition, Biochem Biophys Res Commun, 417 (2012) 576-581.
[20] A. Garcia, R.C. Machado, R.M. Grazul, M.T. Lopes, C.C. Correa, H.F. Dos Santos, M.V. de Almeida, H. Silva, Novel antitumor adamantane-azole gold(I) complexes as potential inhibitors of thioredoxin reductase, J Biol Inorg Chem, 21 (2016) 275-292.
[21] D. Parsonage, F. Sheng, K. Hirata, A. Debnath, J.H. McKerrow, S.L. Reed, R. Abagyan, L.B. Poole, L.M. Podust, X-ray structures of thioredoxin and thioredoxin reductase from Entamoeba histolytica and prevailing hypothesis of the mechanism of Auranofin action, J Struct Biol, 194 (2016) 180-190.
[22] Y. Dong, S.J. Berners-Price, D.R. Thorburn, T. Antalis, J. Dickinson, T. Hurst, L. Qiu, S.K. Khoo, P.G. Parsons, Serine protease inhibition and mitochondrial dysfunction associated with cisplatin resistance in human tumor cell lines: targets for therapy, Biochem Pharmacol, 53 (1997) 1673-1682.

[23] C. Marzano, V. Gandin, A. Folda, G. Scutari, A. Bindoli, M.P. Rigobello, Inhibition of thioredoxin reductase by auranofin induces apoptosis in cisplatin-resistant human ovarian cancer cells, Free Radic Biol Med, 42 (2007) 872-881.
[24] C. Roder, M.J. Thomson, Auranofin: repurposing an old drug for a golden new age, Drugs R D, 15 (2015) 13-20.
[25] M. Navarro, Gold complexes as potential anti-parasitic agents, Coordination Chemistry Reviews, 253 (2009) 1619-1626.
[26] P.I.S. Maia, V.M. Deflon, U. Abram, Gold(III) complexes in medicinal chemistry, Future Medicinal Chemistry, 6 (2014) 1515-1536.
[27] V. Milacic, Q.P. Dou, The tumor proteasome as a novel target for gold(III) complexes: Implications for breast cancer therapy, Coordination Chemistry Reviews, 253 (2009) 1649-1660.
[28] S.J. Berners-Price, A. Filipovska, Gold compounds as therapeutic agents for human diseases, Metallomics, 3 (2011) 863-873.
[29] M.B. Patel, N.R. Modi, J.P. Raval, S.K. Menon, Calix[4]arene based 1,3,4-oxadiazole and thiadiazole derivatives: design, synthesis, and biological evaluation, Org Biomol Chem, 10 (2012) 1785-1794.
[30] Y.T. Li, J.H. Wang, C.W. Pan, F.F. Meng, X.Q. Chu, Y.H. Ding, W.Z. Qu, H.Y. Li, C. Yang, Q. Zhang, C.G. Bai, Y. Chen, Syntheses and biological evaluation of 1,2,3-triazole and 1,3,4-oxadiazole derivatives of imatinib, Bioorg Med Chem Lett, 26 (2016) 1419-1427.
[31] R.R. Somani, P.Y. Shirodkar, Oxadiazole: a biologically active heterocycles, Der Pharma Chemica, 1 (2009) 10.
[32] A.-u.-R. Aziz-ur-Rehman, M. Abbasi, H. Khalid, P. Dar, K. Khan, Synthesis and biological screening of N-substituted derivatives of N-benzyl-4-chlorobenzenesulfonamide, Asian J. Pharm. Hea. Sci, 2 (2012) 384.
[33] M. Miyahara, M. Nakadate, S. Sueyoshi, M. Tanno, M. Miyahara, S. Kamiya, Antitumor activity of 2-acylamino-1,3,4-thiadiazoles and related compounds, Chem Pharm Bull (Tokyo), 30 (1982) 4402-4406.
[34] B. Goswami, J. Kataky, J. Baruah, SYNTHESIS AND BIOLOGICAL-ACTIVITY OF SOME NEW 3-SUBSTITUTED 5-(2, 4-DICHLOROPHENYL)-1, 3, 4-OXADIAZOLE-2-THIONES, in, COUNCIL SCIENTIFIC INDUSTRIAL RESEARCH PUBL & INFO DIRECTORATE, NEW DELHI 110012, INDIA, 1984, pp. 796-797.
[35] K. Manjunatha, B. Poojary, P.L. Lobo, J. Fernandes, N.S. Kumari, Synthesis and biological evaluation of some 1,3,4-oxadiazole derivatives, Eur J Med Chem, 45 (2010) 5225-5233.
[36] C.B. Chapleo, P.L. Myers, A.C. Smith, M.R. Stillings, I.F. Tulloch, D.S. Walter, Substituted 1,3,4-thiadiazoles with anticonvulsant activity. 4. Amidines, J Med Chem, 31 (1988) 7-11.
[37] J.D.S. Chaves, F. Neumann, T.M. Francisco, C.C. Corrêa, M.T.P. Lopes, H. Silva, A.P.S. Fontes, M.V. de Almeida, Synthesis and cytotoxic activity of gold(I) complexes containing phosphines and 3-benzyl-1,3-thiazolidine-2-thione or 5-phenyl-1,3,4-oxadiazole-2-thione as ligands, Inorganica Chimica Acta, 414 (2014) 85-90.
[38] R.R. Somani, P.Y. Shirodkar, Oxadiazole: A biologically important heterocycle, Der Pharma Chemica, 1 (2009) 130-140.
[39] R. Patil, J.S. Biradar, Synthesis and biological activities of new 3,5-disubstituted -2-(ethyl-5'-thioxo-1',3',4'-oxadiazol-4'-ethylacetate-2'-yl)indoles,-2-(5'- thioxo-1',3',4'-oxadiazol-4'methylcarboxyhydrazide-2'-yl) indoles and -2-(5'- thioxo-1',3', 4'-oxadiazol-4'alkyl- 2'-yl) indoles, Indian Journal of Chemistry, 38B (1999) 76-82.
[40] J. Hazarika, J.C.S. Kataky, STUDIES ON BIOLOGICALLY-ACTIVE HETEROCYCLICS - PART VII SYNTHESIS ANDBIOLOGICAL-ACTIVITY OF SOME NEW 3-SUBSTITUTED 5-(2-CHLOROPHENYL)-1,3,4-OXADIAZOL-2-THIONES AND THEIR DERIVATIVES, Indian Journal of Heterocyclic Chemistry, 7 (1998) 197-200.

[41] Shah HP, Shah BR, Bhatt JJ, Desai NC, Undivia N., Synthesis of 2, 5 disubstituted 1, 3, 4-oxadiazoleaspotential antimicrobial, anticancer and HIV agents., Indian Journal of Chemistry, 37B (1998) 180-182.
[42] F. Macaev, G. Rusu, S. Pogrebnoi, A. Gudima, E. Stingaci, L. Vlad, N. Shvets, F. Kandemirli, A. Dimoglo, R. Reynolds, Synthesis of novel 5-aryl-2-thio-1,3,4-oxadiazoles and the study of their structure–anti-mycobacterial activities, Bioorganic & Medicinal Chemistry, 13 (2005) 4842-4850.
[43] V.K.R. Sahu, A.K. Singh, D. Yadav, Review article on 1, 3, 4-Oxadiazole derivaties and it's Pharmacological activities, International Journal of ChemTech Research, 3 (2011) 10.
[44] Z. Trávníček, P. Štarha, J. Vančo, T. Šilha, J. Hošek, P. Suchý, G. Pražanová, Anti-inflammatory Active Gold(I) Complexes Involving 6-Substituted-Purine Derivatives, Journal of Medicinal Chemistry, 55 (2012) 4568-4579.
[45] B. Varnholt, P. Oulevey, S. Luber, C. Kumara, A. Dass, T. Bürgi, Structural Information on the Au–S Interface of Thiolate-Protected Gold Clusters: A Raman Spectroscopy Study, The Journal of Physical Chemistry C, 118 (2014) 9604-9611.
[46] C. Fu, H. Yang, M. Wang, H. Xiong, S. Yu, Serum albumin adsorbed on Au nanoparticles: structural changes over time induced by S-Au interaction, Chemical Communications, 51 (2015) 3634-3636.
[47] A.A. Mohamed, J.A. Krause Bauer, A.E. Bruce, M.R.M. Bruce, [μ-o-Phenylenebis(diphenylphosphine)-κ2P:P′]bis[chlorogold(I)], dppbz(AuCl)2, Acta Crystallographica Section C, 59 (2003) m84-m86.
[48] N. Rösch, A. Görling, D.E. Ellis, H. Schmidbaur, Aurophilicity as Concerted Effect: Relativistic MO Calculations on Carbon-Centered Gold Clusters, Angewandte Chemie International Edition in English, 28 (1989) 1357-1359.
[49] F. Scherbaum, B. Huber, G. Müller, H. Schmidbaur, Use of the CH Acidity of 2,4,4-Trimethyl-4,5-dihydrooxazole to Synthesize Triauriomethanes and Novel Gold Clusters, Angewandte Chemie International Edition in English, 27 (1988) 1542-1544.
[50] N. Lardies, I. Romeo, E. Cerrada, M. Laguna, P.J. Skabara, Synthesis and properties of alkynethiolate gold(i) complexes, Dalton Transactions, (2007) 5329-5338.
[51] R. Narayanaswamy, M.A. Young, E. Parkhurst, M. Ouellette, M.E. Kerr, D.M. Ho, R.C. Elder, A.E. Bruce, M.R.M. Bruce, Synthesis, structure, and electronic spectroscopy of neutral, dinuclear gold(I) complexes. Gold(I)-gold(I) interactions in solution and in the solid state, Inorganic Chemistry, 32 (1993) 2506-2517.
[52] P.P. Tadbuppa, E.R.T. Tiekink, [(Z)-N-Isopropyl-O-methylthiocarbamato-[kappa]S](tri-p-tolylphosphine-[kappa]P)gold(I), Acta Crystallographica Section E, 65 (2009) m1557.
[53] S. Onaka, M. Yaguchi, R. Yamauchi, T. Ozeki, M. Ito, T. Sunahara, Y. Sugiura, M. Shiotsuka, K. Nunokawa, M. Horibe, K. Okazaki, A. Iida, H. Chiba, K. Inoue, H. Imai, K. Sako, The effect of carbon chain length of the diphosphine ligand on the aurophilic interaction. Synthesis and X-ray structural study for a series of Au(I) compounds with Ph2P–R–PPh2 and S-(CH2)n-py ligands, Journal of Organometallic Chemistry, 690 (2005) 57-68.
[54] S. Onaka, Y. Katsukawa, M. Shiotsuka, O. Kanegawa, M. Yamashita, Synthesis, X-ray molecular structure analysis, and study on ligand scrambling reactions of new thiolatogold(I) complexes with various phosphines, Inorganica Chimica Acta, 312 (2001) 100-110.
[55] N.C. Baenziger, W.E. Bennett, D.M. Soborofe, Chloro(triphenylphosphine)gold(I), Acta Crystallographica Section B, 32 (1976) 962-963.
[56] M. Horner, I.C. Casagrande, H. Fenner, J. Daniels, J. Beck, [1,3-Bis(4-nitrophenyl)triazenido](triphenylphosphine)gold(I), Acta Crystallographica Section C, 59 (2003) m424-m426.
[57] S. Bajaj, V. Asati, J. Singh, P.P. Roy, 1,3,4-Oxadiazoles: An emerging scaffold to target growth factors, enzymes and kinases as anticancer agents, European Journal of Medicinal Chemistry, 97 (2015) 124-141.

[58] S.J. Berners-Price, A. Filipovska, Gold compounds as therapeutic agents for human diseases, Metallomics, 3 (2011) 863-873.
[59] M. Vieites, P. Smircich, L. Guggeri, E. Marchan, A. Gomez-Barrio, M. Navarro, B. Garat, D. Gambino, Synthesis and characterization of a pyridine-2-thiol N-oxide gold(I) complex with potent antiproliferative effect against Trypanosoma cruzi and Leishmania sp. insight into its mechanism of action, J Inorg Biochem, 103 (2009) 1300-1306.
[60] V.Z. Mota, G.S. de Carvalho, A.D. da Silva, L.A. Costa, P. de Almeida Machado, E.S. Coimbra, C.V. Ferreira, S.M. Shishido, A. Cuin, Gold complexes with benzimidazole derivatives: synthesis, characterization and biological studies, Biometals, 27 (2014) 183-194.
[61] L. Paloque, C. Hemmert, A. Valentin, H. Gornitzka, Synthesis, characterization, and antileishmanial activities of gold(I) complexes involving quinoline functionalized N-heterocyclic carbenes, Eur J Med Chem, 94 (2015) 22-29.
[62] G. De Muylder, K.K. Ang, S. Chen, M.R. Arkin, J.C. Engel, J.H. McKerrow, A screen against Leishmania intracellular amastigotes: comparison to a promastigote screen and identification of a host cell-specific hit, PLoS Negl Trop Dis, 5 (2011) e1253.
[63] G. Mandal, S. Mandal, M. Sharma, K.S. Charret, B. Papadopoulou, H. Bhattacharjee, R. Mukhopadhyay, Species-specific antimonial sensitivity in Leishmania is driven by post-transcriptional regulation of AQP1, PLoS Negl Trop Dis, 9 (2015) e0003500.
[64] O.L. Fernandez, Y. Diaz-Toro, C. Ovalle, L. Valderrama, S. Muvdi, I. Rodriguez, M.A. Gomez, N.G. Saravia, Miltefosine and antimonial drug susceptibility of Leishmania Viannia species and populations in regions of high transmission in Colombia, PLoS Negl Trop Dis, 8 (2014) e2871.
[65] R. Monte-Neto, M.C. Laffitte, P. Leprohon, P. Reis, F. Frezard, M. Ouellette, Intrachromosomal amplification, locus deletion and point mutation in the aquaglyceroporin AQP1 gene in antimony resistant Leishmania (Viannia) guyanensis, PLoS Negl Trop Dis, 9 (2015) e0003476.
[66] F. Frézard, R. Monte-Neto, P. Reis, Antimony transport mechanisms in resistant leishmania parasites, Biophysical Reviews, 6 (2014) 13.
[67] E.H. Lizarazo-Jaimes, P.G. Reis, F.M. Bezerra, B.L. Rodrigues, R.L. Monte-Neto, M.N. Melo, F. Frézard, C. Demicheli, Complexes of different nitrogen donor heterocyclic ligands with SbCl3 and PhSbCl2 as potential antileishmanial agents against SbIII-sensitive and -resistant parasites, Journal of Inorganic Biochemistry, 132 (2014) 30-36.
[68] C.D. Shaw, J. Lonchamp, T. Downing, H. Imamura, T.M. Freeman, J.A. Cotton, M. Sanders, G. Blackburn, J.C. Dujardin, S. Rijal, B. Khanal, C.J. Illingworth, G.H. Coombs, K.C. Carter, In vitro selection of miltefosine resistance in promastigotes of Leishmania donovani from Nepal: genomic and metabolomic characterization, Mol Microbiol, 99 (2016) 1134-1148.
[69] S. Wyllie, M.L. Cunningham, A.H. Fairlamb, Dual action of antimonial drugs on thiol redox metabolism in the human pathogen Leishmania donovani, J Biol Chem, 279 (2004) 39925-39932.
[70] A.E. Finkelstein, F.R. Roisman, D.T. Walz, Effect of auranofin, a new antiarthritic agent, on immune complex-induced release of lysosomal enzymes from human leukocytes, Inflammation, 2 (1977) 143-150.
[71] R.M. Andrade, J.D. Chaparro, E. Capparelli, S.L. Reed, Auranofin is highly efficacious against Toxoplasma gondii in vitro and in an in vivo experimental model of acute toxoplasmosis, PLoS Negl Trop Dis, 8 (2014) e2973.
[72] R. Diez-Martinez, E. Garcia-Fernandez, M. Manzano, A. Martinez, M. Domenech, M. Vallet-Regi, P. Garcia, Auranofin-loaded nanoparticles as a new therapeutic tool to fight streptococcal infections, Sci Rep, 6 (2016) 19525.
[73] R. Manhas, V.S. Gowri, R. Madhubala, Leishmania donovani Encodes a Functional Selenocysteinyl-tRNA Synthase, J Biol Chem, 291 (2016) 1203-1220.
[74] D.C. Jones, A. Ariza, W.H. Chow, S.L. Oza, A.H. Fairlamb, Comparative structural, kinetic and inhibitor studies of Trypanosoma brucei trypanothione reductase with T. cruzi, Mol Biochem Parasitol, 169 (2010) 12-19.

[75] V. Bhandari, S. Sundar, J.C. Dujardin, P. Salotra, Elucidation of cellular mechanisms involved in experimental paromomycin resistance in Leishmania donovani, Antimicrob Agents Chemother, 58 (2014) 2580-2585.
[76] R. Mukhopadhyay, S. Mukherjee, B. Mukherjee, K. Naskar, D. Mondal, S. Decuypere, B. Ostyn, V.K. Prajapati, S. Sundar, J.C. Dujardin, S. Roy, Characterisation of antimony-resistant Leishmania donovani isolates: biochemical and biophysical studies and interaction with host cells, Int J Parasitol, 41 (2011) 1311-1321.
[77] O.D. Ltd., CrysAlis RED, in, 2008.
[78] G. Sheldrick, A short history of SHELX, Acta Crystallographica Section A, 64 (2008) 112-122.
[79] G. Sheldrick, Crystal structure refinement with SHELXL, Acta Crystallographica Section C, 71 (2015) 3-8.
[80] M.J. Byrnes, M.H. Chisholm, R.J. Clark, J.C. Gallucci, C.M. Hadad, N.J. Patmore, Thienyl carboxylate ligands bound to and bridging MM quadruple bonds, M = Mo or W: models for polythiophenes incorporating MM quadruple bonds, Inorg Chem, 43 (2004) 6334-6344.
[81] Y.G. Sun, B. Jiang, T.F. Cui, G. Xiong, P.F. Smet, F. Ding, E.J. Gao, T.Y. Lv, K. Van den Eeckhout, D. Poelman, F. Verpoort, Solvothermal synthesis, crystal structure, and properties of lanthanide-organic frameworks based on thiophene-2,5-dicarboxylic acid, Dalton Trans, 40 (2011) 11581-11590.
[82] R.H. Blessing, An empirical correction for absorption anisotropy, Acta Crystallogr A, 51 (Pt 1) (1995) 33-38.
[83] L. Farrugia, ORTEP-3 for Windows - a version of ORTEP-III with a Graphical User Interface (GUI), Journal of Applied Crystallography, (1997).
[84] B.M. Sahoo, B.V.V. Ravi Kumar, B.U.B. Prasanna Kumari, Synthesis, characterization and biological evaluation of novel oxadiazole derivatives, International Journal of Pharmaceutical Sciences and Research, 2 (2011) 6.
[85] V. Modi, P. Modi, Oxadiazole: Synthesis, characterization and biological activities, Journal of Saudi Chemical Society, 16 (2012) 327-332.
[86] N.C. Baenziger, W.E. Bennett, D.M. Soborofe, Chloro(triphenylphosphine)gold(I), Acta Crystallographica Section B, 32 (1976) 2.
[87] T. Mosmann, Rapid colorimetric assay for cellular growth and survival: application to proliferation and cytotoxicity assays, J Immunol Methods, 65 (1983) 55-63.
[88] J.A. Joule, K. Mills, Heterocyclic Chemistry, Wiley-Blackwell, Hoboken, N.J, 2010.
[89] S. Habtemariam, In vitro antileishmanial effects of antibacterial diterpenes from two Ethiopian Premna species: P. schimperi and P. oligotricha, BMC Pharmacol, 3 (2003) 6.
[90] M. Ouellette, F. Fase-Fowler, P. Borst, The amplified H circle of methotrexate-resistant leishmania tarentolae contains a novel P-glycoprotein gene, EMBO J, 9 (1990) 1027-1033.
[91] G. Roy, C. Dumas, D. Sereno, Y. Wu, A.K. Singh, M.J. Tremblay, M. Ouellette, M. Olivier, B. Papadopoulou, Episomal and stable expression of the luciferase reporter gene for quantifying Leishmania spp. infections in macrophages and in animal models, Mol Biochem Parasitol, 110 (2000) 195-206.
[92] S.A. Shahzad, M. Yar, Z.A. Khan, I.U. Khan, S.A.R. Naqvi, N. Mahmood, K.M. Khan, Microwave-assisted solvent free efficient synthesis of 1,3,4-oxadiazole-2(3H)-thiones and their potent in vitro urease inhibition activity, 2012, 3 (2012).

List of captions

Figure Captions

Fig. 1. Perspective view of ligand (**D**), ellipsoids are drawn at the 50% probability level and hydrogen atoms are shown as spheres of arbitrary radii.

Fig. 2. Structural perspective of gold(I) complexes. (A, B, C and D) represent complexes (**3-C**), (**4-D**), (**5-E**) and (**8-C**); ellipsoids are drawn at the 50% probability level and some hydrogen atoms were omitted for more clarity. All the ligands used are present in the thiol form.

Fig. 3. Comparative antileishmanial and citotoxicity effect of gold(I) triethylphosphine and triphenylphosphine derivatives. Compounds were assayed against promastigote and amastigote forms of *Leishmania infantum* and *Leishmania braziliensis*. Gold(I) triethylphosphine were selectively more active against amastigote forms of *L. infantum*, however, they also presented higher toxicity against THP-1 cells. The average of IC_{50} values from chloro(triphenylphosphine)gold(I) (black columns – Ph) and chloro(triethylphosphine)gold(I)-derived complexes (grey columns – Et) were obtained from Table 4. Students t test $^{**}p = 0.0017$; $^{***}p = 0.0009$

Fig. 4. Sensitivity profile of *Leishmania guyanensis* wild-type (continuous line) and antimony-resistant *L.* guyanensis (dashed line) to gold(I) triethylphosphine complexes: **(6-A)** (A); **(7-B)** (B); **(8-C)** (C); **(9-D)** (D) and **(10-E)** (E). 5-adamantyl-1,3,4-oxadiazole-2-thione (F) and chloro(triethylphosphine)gold(I)-(G) were used as controls. *L. guyanensis* promastigotes were cultivated in 24-well cell culture plates containing 2 mL of α-MEM medium for 72 h at 25 ºC. The resistant lines were previously selected *in vitro* by step wise drug selection. All data represent average of, at least, two independent experiments. Concentration-response curves were obtained using sigmoidal equation with variable slope on GraphPad Prism 6.0 software RI: Resistance Index

Fig. S1. IR spectra in the 4000-500 cm^{-1} region for ligand (**C**), gold complexes (**3-C**) and (**8-C**)

Fig. S2. ^{1}H NMR spectra in the 8.5-1.0 ppm region for ligand (**D**), gold complexes (**4-D**) and (**9-D**)

Fig. S3. ^{13}C NMR spectra in the 180-10 ppm region for ligand (**D**), gold complexes (**4-D**) and (**9-D**)

Fig. S4. Intermolecular hydrogen bonds for ligand (**D**)

Fig. S5. Intermolecular hydrogen bonds of gold(I) complexes. (A, B, C and D) represent complexes (**3-C**), (**4-D**), (**5-E**) and (**8-C**). Some atoms were deleted for more clarity.

Scheme 1. Schematic representation of the synthesis of gold(I) complexes

Scheme 2. Thione-thiol tautomerization of ligands

Table 1

Crystal data and structure refinement parameters for compounds $C_{10}H_{11}N_3O_4S_2$ (**D**), $C_{26}H_{19}N_2OFPSAu$ (**3-C**), $C_{26}H_{19}N_3O_3PSAu$ (**4-D**), $C_{27}H_{22}N_2O_2PSAu$ (**5-E**) and $C_{14}H_{19}N_2OPSAuF$ (**8-C**).

Compound	**Ligand (D)**	**Complex (3-C)**	**Complex (4-D)**	**Complex (5-E)**	**Complex (8-C)**
Formula	$C_{10}H_{11}N_3O_4S_2$	$C_{26}H_{19}AuFN_2OPS$	$C_{26}H_{19}AuN_3O_3PS$	$C_{27}H_{22}AuN_2O_2PS$	$C_{14}H_{19}AuFN_2OPS$
Formula weight / g mol^{-1}	301.34	654.43	681.44	666.46	510.31
Temperature / K	298(2)	120(2)	120(2)	298 (2)	298(2)
Crystal system	Monoclinic	Monoclinic	Monoclinic	Monoclinic	Triclinic
Space group	*C2/c*	*P2$_1$/n*	*P2$_1$/n*	*C2/c*	*P 1*
a / Å	28.7300(18)	13.6239(4)	13.2854(2)	29.4025(9)	7.8973(2)
b / Å	7.3287(4)	17.9514(5)	18.1873(3)	8.7631(2)	11.0693(3)
c / Å	13.9388(8)	19.5453(5)	20.5524(4)	20.7691(7)	20.5122(5)
α / º	90	90	90	90.00	96.043(2)
β / º	113.442(7)	103.760(3)	103.197(2)	111.930 (4)	100.128(2)
γ / º	90	90	90	90.00	94.847(2)
V / Å^3	2692.6(3)	4643.0(2)	4834.84(15)	4964.1(3)	1745.63(8)
Z	8	8	8	8	4
Crystal size / mm	0.93 x 0.37 x 0.11	0.49 x 0.17 x 0.12	0.23 x 0.12 x 0.06	0.38 x 0.25 x 0.09	0.42 x 0.18 x 0.06
D_{calc}/ g cm^{-3}	1.487	1.872	1.872	1.784	1.942
μ(Mo Kα) / cm^{-1}	0.408	6.526	6.273	6.103	8.647
Transmission factors (min/max)	0.929/0.988	0.979/0.994	0.990/0.997	0.986/0.995	0.960/0.991
Reflections measured / unique	8510/2757	77916/9493	189708/13135	38125/5062	18498/7138
Observed reflections	2182	8086	10706	4228	5561
Nº. of parameters refined	177	595	631	308	379
***R*[F_o>2σ(F_o)]**	0.0415	0.0240	0.0269	0.030	0.0349
***wR*[F_o2>2σ(F_o)^2]**	0.1169	0.0440	0.0426	0.059	0.0690
S	1.036	1.093	1.050	1.045	1.048
RMS peak/	0.046	0.119	0.135	0.079	0.162

Table 2

Selection of the main geometric parameters, bond distance and bond angles to the (**D**) ligand and (**3-C**), (**4-D**), (**5-E**) and (**8-C**) complexes.

Ligand (D)			
	Bond distance (Å)		
S2—C1	1.643 (2)	O1—C2	1.367 (2)
O1—C1	1.376 (2)	O4—S2	1.5006 (17)
C6—N3	1.473 (3)	C1—N1	1.325 (3)
N3—O2	1.220 (3)	N1—N2	1.379 (2)
N2—C2	1.282 (2)	O3—N3	1.214 (3)
C9—S2	1.770 (3)	C10—S2	1.761 (3)
	Bond angle(º)		
C2—O1—C1	105.95 (14)	C7—C6—N3	118.62 (17)
N1—C1—O1	104.98 (17)	C5—C6—N3	118.75 (17)
N1—C1—S1	131.33 (17)	O5—N3—O2	123.3 (2)
O1—C1—S1	123.69 (14)	O3—N3—C6	118.56 (19)
C1—N1—N2	112.47 (17)	O2—N3—C6	118.14 (19)
C2—N2—N1	103.75 (15)	N2—C2—O1	112.85 (15)
O4—S2—C10	106.57 (12)	N2—C2—C3	128.18 (16)
O4—S2—C9	105.67 (12)	O1—C2—C3	118.96 (15)
C10—S2—C9	98.30 (16)		
Complex (3-C)			
	Bond distance (Å)		
Au1A—P1A	2.2584 (9)	Au1A—S1A	2.3137 (9)
Au1A—Au1	3.1189 (2)	Au1—P1	2.2531 (9)
Au1—S1	2.3143 (9)		
	Bond angle(º)		
P1—Au1—S1	173.42 (3)	P1A—Au1A—S1A	168.93 (3)
Complex (4-D)			
	Bond distance (Å)		
Au1—P1	2.2551 (7)	Au1—S1	2.3132 (7)
Au1—Au1A	3.1545 (1)	Au1A—P1A	2.2559 (7)
Au1A—S1A	2.3147 (7)		
	Bond angle(º)		
P1A—Au1A—S1A	173.95 (3)	P1—Au1—S1	171.59 (2)
Complex (5-E)			
	Bond distance (Å)		
Au1—P1	2.2609 (11)	Au1—S1	2.2991 (13)
	Bond angle(º)		
	P1—Au1—S1	179.01 (5)	
Complex (8-C)			
	Bond distance (Å)		
Au1A—P1A	2.2602 (13)	Au1A—S1A	2.3220 (14)
Au1A—Au1	3.0573 (3)	Au1—P1	2.2447 (19)
	Bond angle(º)		
P1—Au1—S1	176.78 (7)	P1A—Au1A—S1A	175.10 (5)

Table 3

Anticancer activity against tumoral and non tumoral cell lines.

Compound	IC_{50} (μM ± SD)				
	Tumor cells				Non tumor cells
	B16F10	**SI[b]**	**CT26.WT**	**SI[b]**	**BHK-21**
(**A**) Ligand	6.53±0.60	12.8	8.28±0.40	10.10	83.60±1.00
(**B**) Ligand	4.30±0.50	14.74	66.87±1.10	0.95	63.4±1.30
(**C**) Ligand	>100.00	1.00	<0.10	>1000.00	>100.00
(**D**) Ligand	0.26±0.10	42.70	1.89±0.20	5.87	11.1±0.10
(**E**) Ligand	>100.00	1.00	53.74±1.00	>1.86	>100.00
(**1-A**)	0.12±0.03	27.9	<0.10	33.50	3.35±0.50
(**2-B**)	<0.10	>68.80	1.66±0.10	4.14	6.88±0.20
(**3-C**)	1.40±0.50	5.06	<0.10	>70.80	7.08±0.50
(**4-D**)	0.14±0.10	13.00	1.43±0.20	1.27	1.82±0.20
(**5-E**)	1.01±0.20	2.02	0.48±0.10	4.25	2.04±0.10
(**6-A**)	0.18±0.05	34.2	0.40±0.04	15.40	6.15±0.20
(**7-B**)	<0.10	>2.30	0.23±0.10	1.00	0.23±0.10
(**8-C**)	0.43±0.30	0.77	<0.10	>3.30	0.33±0.10
(**9-D**)	<0.10	>19.20	0.51±0.10	3.76	1.92±0.20
(**10-E**)	0.18±0.20	15.90	0.36±0.10	7.94	2.86±0.10
$Au(PPh_3)Cl$	0.90±0.10	5.70	1.76±0.10	3.74	6.59±0.20
$Au(PEt_3)Cl$	0.50±0.10	14.18	1.80±0.10	3.94	7.09±0.30
Cisplatin	6.40±2.20	1.30	0.70±0.20	12.0	8.40±1.90

SD: standard deviation of triplicate of two independent experiments.
[b] SI – selectivity index.

Table 4 Antileishmanial activity of gold(I) derivatives against *Leishmania* promastigote and intracelular amastigote forms. Selectivity indexes are shown based on cytotoxic activity performed on THP-1 macrophages.

Compound	**CC_{50} (µM) (95% CI)**	**IC_{50} (µM) (95% CI) prom.**		**SI prom.**		**IC_{50} (µM) Int. ama.**	**SI ama.**
	THP-1 MΦ	***L. infantum***	***L. braziliensis***	***Li***	***Lb***	***L. infantum***	***Li***
(A) Ligand	> 50	> 100	> 100			ND	
(B) Ligand	> 50	> 100	> 100			ND	
(C) Ligand	> 50	> 100	> 100			ND	
(D) Ligand	> 50	27.56 (21.94-34.63)	32.4 (29.47-35.62)	> 1.81	> 1.54	ND	
(E) Ligand	> 50	> 100	> 100			ND	
(1-A)	11.54 (10.89-12.23)	4.69 (3.92-5.60)	7.03 (6.38-7.74)	2.46	1.64	2.98 (2.66-3.33)	3.87
(2-B)	10.67 (10.02-11.38)	4.75 (3.99-5.66)	6.46 (5.98-6.96)	2.24	1.65	2.76 (2.11-3.61)	3.86
(3-C)	8.46 (7.97-8.98)	3.89 (3.16-4.78)	5.68 (5.22-6.18)	2.17	1.5	3.71 (2.94-4.7)	2.28
(4-D)	10.7 (9.45-12.11)	4.66 (3.92-5.53)	9.17 (8.37-10.06)	2.3	1.16	3.64 (3.08-4.31)	2.93
(5-E)	11.12 (10.46-11.82)	6.15 (5.32-7.11)	8.34 (7.5-9.27)	1.8	1.33	4.25 (3.86-4.68)	2.61
(6-A)	4.41 (3.65-5.32)	4.02 (3.75-4.31)	7.2 (6.63-7.8)	1.09	0.61	0.97 (0.82-1.14)	4.54
(7-B)	7.84 (6.62-9.3)	6.85 (6.59-7.13)	10.57 (9.96-11.21)	1.14	0.74	1.7 (1.4-2-2)	4.61
(8-C)	6.7 (6.12-7.34)	2.73 (2.31-3.23)	4.69 (4.4-5.01)	2.45	1.42	2.21 (1.82-2.68)	3.03
(9-D)	6.37 (5.48-7.41)	5.38 (5.17-5.6)	9.27 (8.33-10.33)	1.18	0.68	1.41 (1.16-1.71)	4.51
(10-E)	7.05 (6.32-7.86)	3.41 (2.86-4.08)	4.89 (4.58-5.23)	2.06	1.44	2.41 (1.95-3)	2.92
$Au(PPh_3)Cl$	4.98 (4.64-5.33)	4.53 (3.91-5.26)	5.25 (4.65-5.93)	1.09	0.94	0.9 (0.58-1.36)	5.53
$Au(PEt_3)Cl$	5.43 (5.08-5.79)	1.94 (1.61-2.33)	2.79 (2.51-3.10)	2.8	1.94	1.35 (1.15-1.60)	3.77
AmB	12 (11.43-12.59)	0.1 (0.1-0.11)	0.1 (0.09-0.11)	120	120	0.09 (0.08-0.09)	133
Miltefosine	39.08 (37.65-40.57)	ND	ND	ND	ND	0.57 (0.54-0.60)	68.56

SI: selectivity index; CI: confidence interval; IC_{50}: inhibitory concentration that reduces 50% of cellular growth; CC: cytotoxic concentration that reduces cellular viability by 50%; prom: promastigote forms; Int. Ama: intracellular amastigotes; $Au(PPh_3)Cl$: chloro(triphenylphosphine)gold(I); $Au(PEt_3)Cl$: chloro(triethylphosphine)gold(I); AmB: amphotericin B; not determined

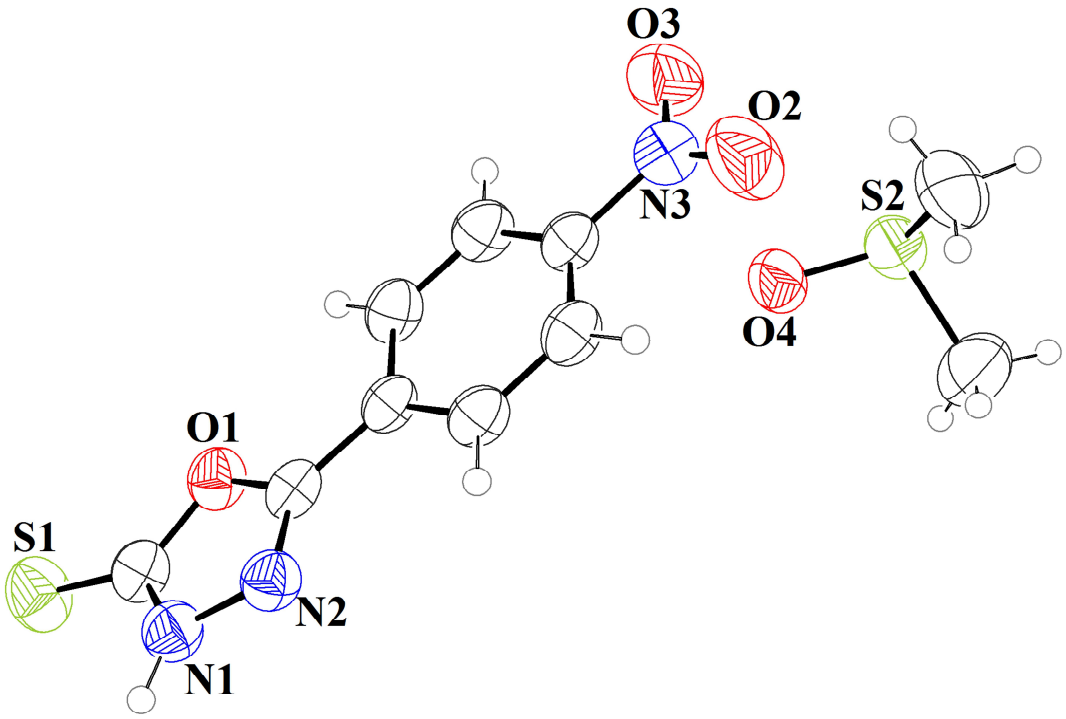

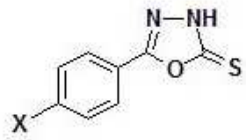

(A) X = H
(B) X = Cl
(C) X = F
(D) X = NO_2
(E) X= OCH_3

+ $Au(PR_3)Cl$

R = Et
R= Ph

r.t, 9 h, in the dark

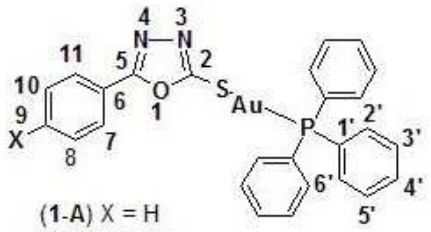

(**1**-A) X = H
(**2**-B) X = Cl
(**3**-C) X = F
(**4**-D) X = NO_2
(**5**-E) X= OCH_3

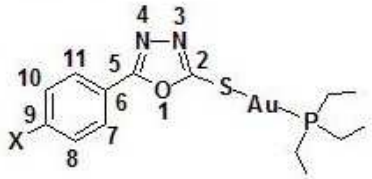

(**6**-A) X = H
(**7**-B) X = Cl
(**8**-C) X = F
(**9**-D) X = NO_2
(**10**-E) X= OCH_3

A

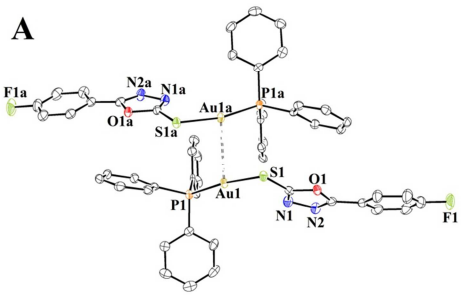

Complex (3-C)

B

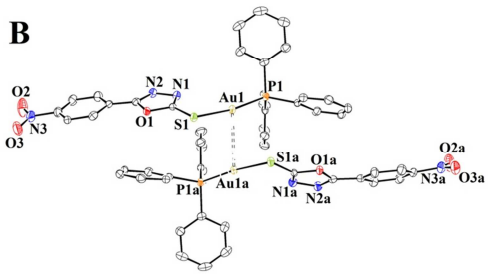

Complex (4-D)

C

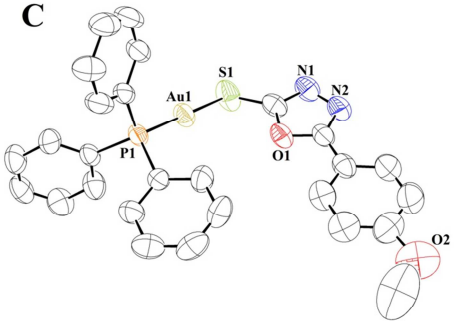

Complex (5-E)

D

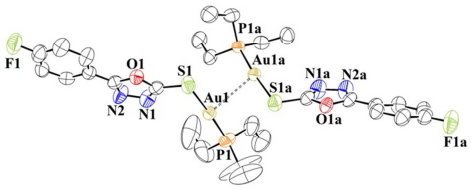

Complex (8-C)

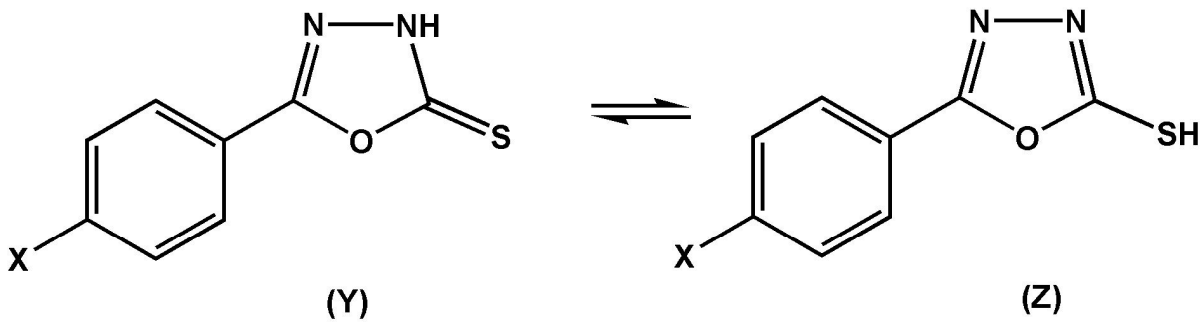

(**A**) X = H
(**B**) X = Cl
(**C**) X = F
(**D**) X = NO_2
(**E**) X= OCH_3

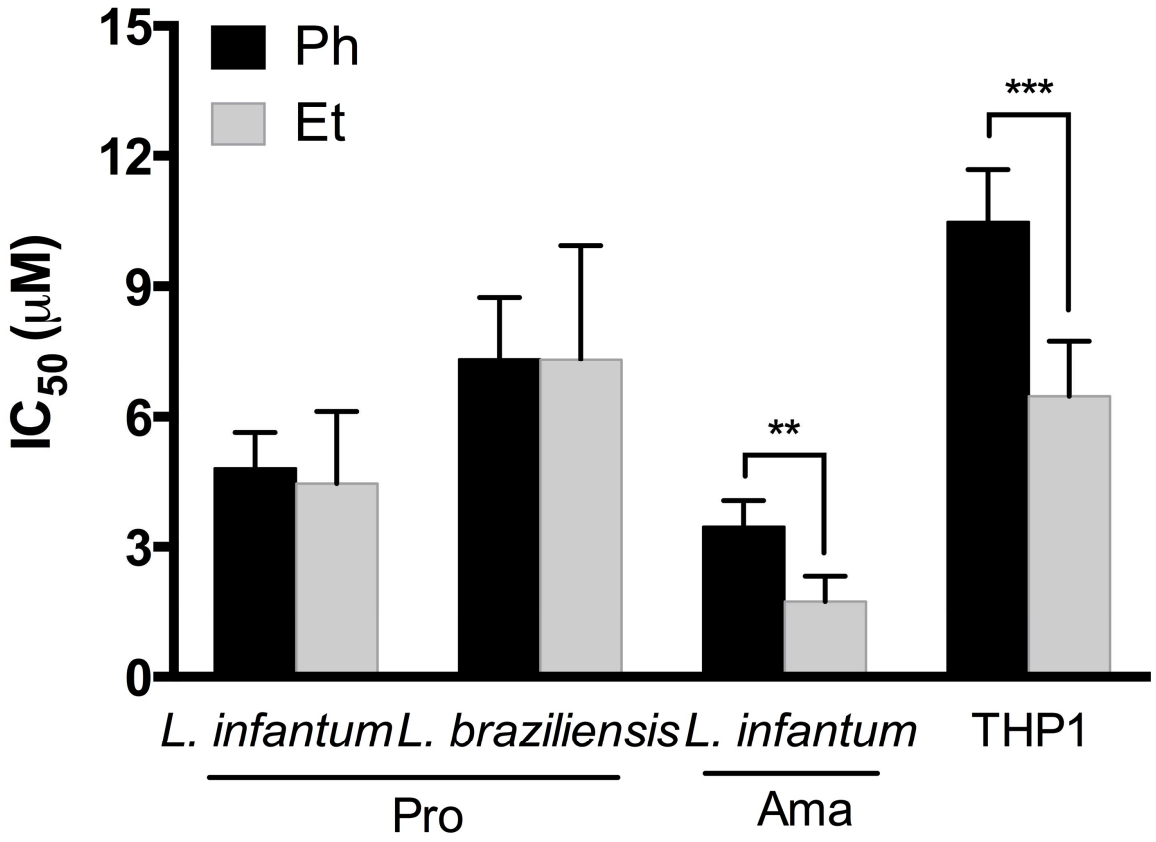

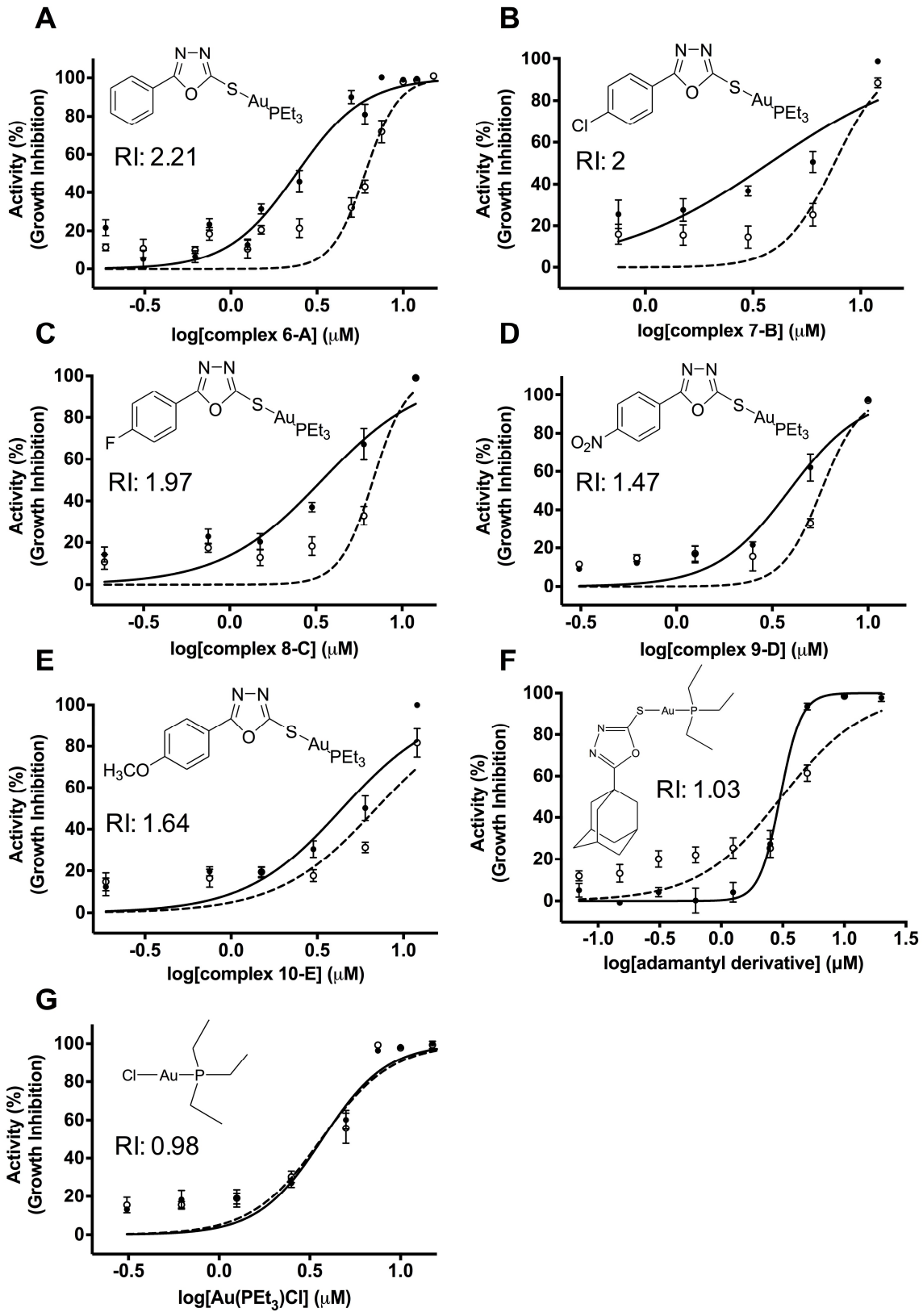
A
RI: 2.21
Activity (%) (Growth Inhibition)
log[complex 6-A] (μM)
B
RI: 2
log[complex 7-B] (μM)
C
RI: 1.97
log[complex 8-C] (μM)
D
RI: 1.47
log[complex 9-D] (μM)
E
RI: 1.64
log[complex 10-E] (μM)
F
RI: 1.03
log[adamantyl derivative] (μM)
G
RI: 0.98
log[Au(PEt3)Cl] (μM)

Highlights

Gold(I) complexes are active against cancer cell lines and *Leishmania* parasites.

Most compounds were more active than cisplatin against B16F10 and CT26.WT cell lines.

Compound (**6-A**) was very selective against colon cancer CT26.WT cell line.

Gold(I) complexes can be applied to better understand drug resistance in *Leishmania.*

.